

---

# Transformer Key-Value Memories Are Nearly as Interpretable as Sparse Autoencoders

---

**Mengyu Ye**  
Tohoku University  
ye.mengyu.s1@dc.tohoku.ac.jp

**Jun Suzuki**  
Tohoku University & RIKEN  
jun.suzuki@tohoku.ac.jp

**Tatsuro Inaba\***  
MBZUAI  
tatsuro.inaba@mbzuai.ac.ae

**Tatsuki Kuribayashi**  
MBZUAI  
tatsuki.kuribayashi@mbzuai.ac.ae

## Abstract

Recent interpretability work on large language models (LLMs) has been increasingly dominated by a feature-discovery approach with the help of proxy modules. Then, the quality of features *learned* by, e.g., sparse auto-encoders (SAEs), is evaluated. This paradigm naturally raises a critical question: do such learned features have better properties than those *already represented* within the original model parameters, and unfortunately, only a few studies have made such comparisons systematically so far. In this work, we revisit the interpretability of feature vectors stored in feed-forward (FF) layers, given the perspective of FF as key-value memories, with modern interpretability benchmarks. Our extensive evaluation revealed that SAE and FFs exhibits a similar range of interpretability, although SAEs displayed an observable but minimal improvement in some aspects. Furthermore, in certain aspects, surprisingly, even vanilla FFs yielded better interpretability than the SAEs, and features discovered in SAEs and FFs diverged. These bring questions about the advantage of SAEs from both perspectives of feature quality and faithfulness, compared to directly interpreting FF feature vectors, and FF key-value parameters serve as a strong baseline in modern interpretability research<sup>2</sup>.

## 1 Introduction

Transformer-based language models (LMs) have exhibited outstanding performance on a wide variety of tasks [10, 35, 1, 44, 45], whereas their underlying mechanisms remain opaque [47, 37, 50, 17, 38, 18, 34, 28, 31]. This issue has been tackled in the interpretability field, and in earlier days, the field has typically adopted a *top-down* approach, where, given candidate features or algorithms, e.g., syntactic structure, it has been inspected where in the original model those are encoded. Nowadays, as a variety of capabilities emerge in larger LMs, the question tends to be more on the *bottom-up*, feature-discovery side: what kind of features are encoded in the model?; and how can we discover and control them? This feature-discovery age has brought two trends to the interpretability community simultaneously: (i) training an external proxy module dedicated to this purpose, namely, sparse auto-encoder (SAEs), to decompose neuron activations into simpler basic features [53, 8, 24, 30, 21, 16] (**proxy-based analysis**), and (ii) developing new comprehensive interpretability benchmarks [36, 27] to test the quality of discovered features.

This paper explores one overlooked question in the field, to what extent a proxy-based, *artificial* decomposition of neuron activations empirically benefits the model interpretation. In other words,

---

\*Work done at Tohoku University.

<sup>2</sup>Project page: <https://muyo8692.com/projects/ff-kv-sae>

feed-forward (FF) layers naturally implement the decomposition of neural activation into a set of feature vectors, through the lens of FF as key-value memories [17](**FF-KV analysis**), why not first evaluate such *organic* features in FFs with the newly developed interpretability benchmarks? Proxy-based and FF-KV analysis have complementary advantages, and thus, there is no immediate reason to dismiss the latter. For example, while some proxy-based methods have a theoretical motivation to handle superposition, they also have limitations that FF-KV analysis can automatically bypass: proxy modules can additionally expose biases to the interpretation, e.g., specific features are repeatedly found [8, 49, 11]; the external proxy hallucinates features [22]; and additional computation costs are needed to interpret the model. Furthermore, the FF activations are reported to be naturally sparse even without any regularization [29]. Thus, if FF-KV and SAE analyses yield comparable results, there are several advantages (more simply put, from Occam’s Razor principle) to adopting the former FF-KV analyses.

To gauge the (dis)similarities between FF-KVs’ and SAEs’ interpretability level, we perform both automatic evaluation and manual feature analyses. Automatic evaluation with SAEBENCH demonstrates surprising similarities between the two approaches. The evaluation scores fell into a similar range in all eight metrics in SAEBENCH, and the inter-metrics tendencies are also paralleled, e.g., causal intervention scores are poorer than feature disentanglement scores in both methods. One can even observe some advantages of FF-KVs; for example, features in the original FFs tend to avoid feature overlapping, resulting in better absorption scores [11] (i.e., less redundancy) than those in SAEs. These comparable quality is further supported by human manual evaluation of feature qualities. Conceptual features can be found with almost equal ease from both FF-KV features and SAEs. These tentatively conclude that features from FF-KVs and SAEs serve a quite similar level of interpretability from both quantitative and qualitative perspectives.

In our analysis, we further investigate the faithfulness of proxy-discovered features, considering FF-KV features as gold, how large is the overlap between the feature sets of the original FF-KV module and that of the proxy module? We analyzed such an overlap with Transcoder (TC), the closest counterpart to FF-KV, as a proxy model, and revealed that the majority of TC features do not have similar counterparts in the original FF module. This aligns with the existing report that SAEs can interpret even random Transformers [22], and perhaps the proxy module hallucinates new features rather than translating the workings of the original FF module, encouraging further research on the faithfulness of the learned features, with FF-KV features as grounding points. To sum up, our study reveals that proxy-based methods such as SAEs empirically offer very limited advantage over the direct analysis of FFs (i.e., key-value memories). That is, the theoretical advantage of SAEs is not observed empirically, at least through the lens of the current evaluation scheme, and encourages the inclusion of FF-KV features as a strong baseline when assessing feature-discovery methods in the interpretability field.

## 2 Background

### 2.1 Related Work

**Dictionary Learning and LLMs Interpretation.** Dictionary learning has been proposed to address polysemanticity of the representation [3, 52, 42, 40, 14, 5, 20], and this has been applied to interpret the internal activations of LLMs, represented by sparse autoencoders (SAEs) [53, 8, 24, 30, 21, 16, 25]. Specifically, these introduce a proxy module to decompose and reconstruct a model’s activation, and seek interpretable features in it. Apparently, promising results were observed in earlier days: the learned features are highly interpretable and can be directly used to steer the model’s behavior [46]: modification on a feature will either eliminate the corresponding behavior, or enhance it.

**Mixed Reports on SAE Features.** Although the SAEs get increasing attention, concurrent works have brought skeptical views on their success. For example, SAE-based feature steering quality is inferior to simple baselines utilizing activations [51]; SAEs can learn meaningful features even from a randomly initialized Transformer [22]; and they exhibit no clear advantage in downstream tasks and sometimes underperform linear probes that use the model’s raw activations [9, 26]. This study, at a high level, provides additional support for such criticisms of the general advantage of SAEs.

**Interpretability of Feed-Forward (FF) Layers.** There have been a fair number of studies to interpret the feed-forward (FF) layer in Transformers directly [13, 40, 2]. The closest work to ours

is Geva et al. [17], where FFs can be viewed as key-value memories, and they are interpretable and useful to control the model output. Recent work also indicates that activations in FFs are already sparse [29], and their neurons can be manipulated [51]; these motivate our work to contextualize the bare FF interpretability with SAE works.

## 2.2 Sparse Autoencoder for Transformer Interpretability

**Transformer.** Transformer architecture is a stack of multiple modules, such as attention mechanisms, feed-forward (FF) layers, and normalization layers. There have recently been increasing endeavors to interpret, especially, neuron activations around FF layers, such as SAEs. Henceforth, vector denotes a row vector.

**SAE.** SAE decomposes and reconstructs the neuron activations, typically after the FF layer (residual stream). That is, let  $\mathbf{x}_{\text{FF}_{\text{out}}} \in \mathbb{R}^{d_{\text{model}}}$  be neuron activations after the FF layer, and  $d_{\text{SAE}}$  denotes the dimension of SAE features. SAE decomposes the neuron activations  $\mathbf{x}_{\text{FF}_{\text{out}}}$  and reconstructs it  $\hat{\mathbf{x}}_{\text{FF}_{\text{out}}}$  as follows:

$$\hat{\mathbf{x}}_{\text{FF}_{\text{out}}} \approx \text{ReLU}(\mathbf{x}_{\text{FF}_{\text{out}}} \mathbf{W}_{\text{enc}} + \mathbf{b}_{\text{enc}}) \mathbf{W}_{\text{dec}} + \mathbf{b}_{\text{dec}}, \quad (1)$$

with  $\mathbf{W}_{\text{enc}} \in \mathbb{R}^{d_{\text{model}} \times d_{\text{SAE}}}$ ,  $\mathbf{W}_{\text{dec}} \in \mathbb{R}^{d_{\text{SAE}} \times d_{\text{model}}}$ ,  $\mathbf{b}_{\text{enc}} \in \mathbb{R}^{d_{\text{SAE}}}$ , and  $\mathbf{b}_{\text{dec}} \in \mathbb{R}^{d_{\text{model}}}$  in the SAE module.  $\text{ReLU}(\cdot) : \mathbb{R}^d \rightarrow \mathbb{R}^d$  denotes an element-wise ReLU activation. Each **activation** dimension is treated as a potentially interpretable feature, and the **matrix** maps each feature dimension to its feature vector in the representation space. This module is trained so that the activations are as sparse as possible with a sparsity loss to disentangle the potentially polysemantic input neurons.

**Transcoder.** Notably, as an alternative to SAEs and perhaps the closest attempt to this study, *Transcoders* have recently been proposed [12]. This approximates the original FF by training a sparse MLP as a proxy to predict FF output  $\mathbf{x}_{\text{FF}_{\text{out}}}$  from FF input  $\mathbf{x}_{\text{FF}_{\text{in}}}$ , and its internal activations ( $\in \mathbb{R}^{d_{\text{TC}}}$ ) are evaluated in the same way as the standard SAE. Still, their work [12] did not clearly evaluate how interpretable the original FF’s internal activations are, and this work complements this overlooked question.

## 2.3 Feed-Forward Layer as Key-Value Memories

Feed-forward layers in Transformers once project the FF input  $\mathbf{x}_{\text{FF}_{\text{in}}} \in \mathbb{R}^{d_{\text{model}}}$  to  $d_{\text{FF}}$ -dimensional representation ( $d_{\text{model}} < d_{\text{FF}}$ ), applies an element-wise non-linear activation  $\phi(\cdot) : \mathbb{R}^d \rightarrow \mathbb{R}^d$ , and projects it back, as follows:

$$\mathbf{x}_{\text{FF}_{\text{out}}} = \phi(\mathbf{x}_{\text{FF}_{\text{in}}} \mathbf{W}_K + \mathbf{b}_K) \mathbf{W}_V + \mathbf{b}_V = \sum_{i \in d_{\text{FF}}} \phi(\mathbf{x}_{\text{FF}_{\text{in}}} \mathbf{W}_K)_{[i]} \mathbf{W}_V_{[:,i]} + \mathbf{b}_V, \quad (2)$$

where  $\mathbf{W}_K \in \mathbb{R}^{d_{\text{model}} \times d_{\text{FF}}}$  and  $\mathbf{W}_V \in \mathbb{R}^{d_{\text{FF}} \times d_{\text{model}}}$  are learnable weight matrices, and  $\mathbf{b}_K \in \mathbb{R}^{d_{\text{FF}}}$ ,  $\mathbf{b}_V \in \mathbb{R}^{d_{\text{model}}}$  are learnable biases.  $d_{\text{FF}}$  is typically set as  $4d_{\text{model}}$ . One interpretation of the FF layer is a knowledge retrieval module; that is, the module first creates **keys (activations)** from an input  $\mathbf{x}_{\text{FF}_{\text{in}}}$  and then aggregates their associated **values (feature vectors)**. Existing studies have analyzed what kind of concept is stored in each feature vector of  $\mathbf{W}_V_{[:,i]}$  and when they are activated by  $\phi(\mathbf{x}_{\text{FF}_{\text{in}}} \mathbf{W}_K)_{[i]}$  [17].

## 3 Comparing FF-KVs with SAEs

The feed-forward key-value memory module (FF-KV) inherently performs the same operation as SAEs (although it is somewhat obvious, given that both adopt the MLP architectures): it first decomposes the neuron activations into feature vectors and then aggregates them. This naturally raises a question about how similar the decomposition *naturally* made by FF-KVs is to that *learned* by the proxy module, e.g., SAEs. We examine several variants of FF-KV-based feature discovery methods<sup>3</sup>.

<sup>3</sup>See Appendix A for the details on the implementations

### 3.1 Methods

**FF-KV.** The vanilla FF key-value memories are evaluated with the SAE evaluation framework, treating the **key activations** as features and the **value vectors** as feature vectors.

**TopK FF-KV.** To encourage the alignment with SAE research, we also introduce sparsity to activations in FFs by applying a top- $k$  activation function to the key vector, although it has been reported that the vanilla FFs’ activations are somewhat already sparse [29]. This keeps only the  $k$  neurons with the  $k$  largest activations in each inference, zeroing out the activation for the rest. We call this **TopK FF-KV**, defined as follows:

$$\mathbf{x}_{\text{FF}_{\text{out}}} \approx \text{Top-}k(\phi(\mathbf{W}_K \mathbf{x}_{\text{FF}_{\text{in}}} + \mathbf{b}_K)) \mathbf{W}_V + \mathbf{b}_V . \quad (3)$$

**Normalized FF-KV.** The feature vectors of SAE are typically normalized, whereas those in FF are not. If a particular feature vector  $\mathbf{W}_{V[i,:]}$  has a large norm, the magnitude of its corresponding activation may be underestimated. To handle this potential concern, we normalize each row of  $\mathbf{W}_V$ , and the discounted vector norm is weighted to activations. We refer to the method with this post-correction as **Normalized (TopK) FF-KV**:

$$\mathbf{x}_{\text{FF}_{\text{out}}} \approx \text{Top-}k(\phi(\mathbf{W}_K \mathbf{x}_{\text{FF}_{\text{in}}} + \mathbf{b}_K) \odot \mathbf{s}) \tilde{\mathbf{W}}_V + \mathbf{b}_V , \quad (4)$$

$$\mathbf{s} = [\|\mathbf{W}_{V[1,:]} \|_2, \|\mathbf{W}_{V[2,:]} \|_2, \dots, \|\mathbf{W}_{V[d_{\text{FF}},:]} \|_2] \in \mathbb{R}^{d_{\text{FF}}} . \quad (5)$$

Here,  $\tilde{\mathbf{W}}_V = \text{diag}(\mathbf{s})^{-1} \mathbf{W}_V$ , where  $\text{diag}(\cdot)$  expands a vector  $\mathbb{R}^d$  to a diagonal matrix  $\mathbb{R}^{d \times d}$ .

### 3.2 Inference and Feature Discovery

Once a method to obtain activations from the models is determined, one can get an activation history over a certain set of text. Here, we introduce several notations before going to the experiments.

**Notations.** Feature activations are analyzed through feeding specific texts to models, and the exact text contents will vary depending on evaluation metrics. Let us denote a set of input texts as  $\mathcal{S} = [\mathbf{s}_1, \dots, \mathbf{s}_n]$ , where each text consists of multiple tokens  $\mathbf{s}_k = [w_{(k,1)}, w_{(k,2)}, \dots, w_{(k,m)}] \in \mathcal{S}$ , which are used to get feature activations. For brevity, we flatten and re-index the tokens as  $[w_1, w_2, \dots, w_l]$ ; one can recover the original indices  $(i, j)$  indicating text id and token position via  $\sigma : \mathbb{N}_{[1,l]} \rightarrow \mathbb{N}_{[1,n]} \times \mathbb{N}_{[1,m]}$ , e.g.,  $\sigma(2) = (1, 2)$ . For each token  $w_t$ , we first collect feature activations  $\mathbf{a}_t \in \mathbb{R}^{d_{\text{coder}}}$  with a particular method, such as SAE. Here,  $d_{\text{coder}}$  should be  $d_{\text{SAE}}$ ,  $d_{\text{TC}}$ , or  $d_{\text{FF}}$ , depending on the methods; in other words, each method can maximally yield  $d_{\text{coder}}$  numbers of features  $\mathcal{F} = [f_1, \dots, f_{d_{\text{coder}}}]$ . Repeatedly collecting the activations over inputs  $[w_1, \dots, w_l]$  gives an activation history matrix  $A \in \mathbb{R}^{l \times d_{\text{coder}}}$ , where each row corresponds to each token  $x_t$ , and each column corresponds to each feature (neuron)  $f_p \in \mathcal{F}$ , respectively.  $A_{[:,p]} \in \mathbb{R}^l$  presents where a feature  $f_p$  was activated in  $\mathcal{S}$ .  $\mathcal{S}_p = \{t_i \in T \mid A_{t,p} > 0 \text{ and } i, _ = \sigma(t)\} \subseteq \mathcal{S}$  represents the text subset associated with the feature  $f_p$ .

**SwiGLU activation.** Modern LMs adopt a SwiGLU gating function [41] for the non-linear activation of FFs  $\phi(\cdot)$ . The existing work [54] showed the compatibility of SwiGLU activation with FF-KV analysis, and thus, the above methods (§ 3.1) can be naturally implemented with SwiGLU. For example, on top of the SwiGLU activation, the TopK FF-KV can be written as follows:

$$\mathbf{x}_{\text{FF}_{\text{out}}} \approx \text{Top-}k((\mathbf{W}_G \mathbf{x}_{\text{FF}_{\text{in}}}) \odot \text{Swish}(\mathbf{W}_K \mathbf{x}_{\text{FF}_{\text{in}}})) \mathbf{W}_V + \mathbf{b}_V , \quad (6)$$

$$= \sum_{i \in d_{\text{FF}}} \text{Top-}k((\mathbf{W}_G \mathbf{x}_{\text{FF}_{\text{in}}}) \odot \text{Swish}(\mathbf{W}_K \mathbf{x}_{\text{FF}_{\text{in}}}))_{[i]} \mathbf{W}_{V[:,i]} + \mathbf{b}_V , \quad (7)$$

where,  $\mathbf{W}_G \in \mathbb{R}^{d_{\text{FF}} \times d_{\text{model}}}$  is the gating matrix.

## 4 Experiment 1: Automatic Evaluation

We evaluate FF-KVs, SAEs, and Transcoders using the metrics from SAE BENCH [27]. We also report the Feature Alive Rate as a complementary statistic.

## 4.1 Evaluation Metrics

Here, we give a high-level description of each metric, and details are shown in Appendix B.

**Feature Alive Rate** aggregates how many features are alive, out of  $d_{\text{coder}}$  features. A positive value of  $A_{t,p}$  is regarded as the activation of  $p$ -th feature in  $x_t$ . An indicator function,  $\chi : X_{[:,p]} \mapsto 1$  if  $\max(X_{[:,p]}) > 0$  else 0, judges if the feature  $f_p$  is *alive* (activated at least once) and the following score is calculated:  $\frac{\sum_{j=1}^{d_{\text{coder}}} \chi(A_{t,j})}{d_{\text{coder}}}$ . A score of 1 indicates that all features are activated at least once.

**Explained Variance** evaluates how well the proxy module reconstructs the original activations, and the FF-KV methods (without proxies) can automatically get a perfect score (=1) since this is the original module as is.

**Absorption Score** evaluates how many features a particular simple concept (e.g., word starting with ‘‘S’’) is split into. A higher value implies that many features are needed to emulate the targeted single concept, and thus, the feature set is redundant.

**Sparse Probing** evaluates the existence of specific informative features (e.g., sentiment) and their generalizability to held-out data. This is measured based on the accuracy of probe classifiers trained on the activation patterns to predict the properties of unseen inputs for the proxy module.

**Auto-Interpretation Score** evaluates how easily the activation patterns of the feature can be summarized in natural language (e.g., ‘‘a feature related to accounting’’). Specifically, given a text subset  $S_p$  for the feature  $f_p$ ,<sup>4</sup> an LLM is requested to summarize the feature concept and then predict the (binary) feature activation on the held-out set based on the summary, following Paulo et al. [36]. A score of 1 indicates that features can be perfectly summarized, and their activations are predictable.

**Spurious Correlation Removal (SCR)** evaluates how well spuriously correlated two features (e.g., gender and profession) are disentangled from different features, using the SHIFT [32] data. A score of 1 indicates a perfect disentanglement. Notably, its extension, Targeted Probe Perturbation (TPP) score, was also invented as a supplemental metric in SAEBENCH [27]. The TPP results are shown in Appendix and yielded consistent results with SCR. Notably, SCR and TPP consider top- $K$  activations in evaluations (we adopt  $K = 20$  here, following existing studies [27])<sup>5</sup>, and results for different  $K$  are shown in Appendix B.

**RAVEL** [23] further evaluates the feature overlap and disentanglement, but slightly from a different angle from SCR and TPP. Specifically, this concerns the separability and controllability of multiple different attributes of the same entity (e.g., Japan  $\xrightarrow{\text{continent}}$  Asia, Japan  $\xrightarrow{\text{capital}}$  Tokyo). The RAVEL score can be decomposed into two complementary scores: (i) Isolation score—the probability that all non-edited attributes remain unchanged; and (ii) Causality score—the probability that the edit successfully changes the target attribute. We report both scores for the RAVEL results to clarify the fine-grained properties.

## 4.2 LMs and Proxy Modules

**LMs.** We evaluate FFs in all layers of five LMs: Gemma-2-2B, Gemma-2-9B [43], Llama-3.1-8B [45], GPT-2 [39], and Pythia-70M [4]. Due to space limitations, the results of the middle layers of Gemma-2-2B (layer 13) and Llama-3.1-8B (layer 16) are shown in the main part of this paper, and the results for other layers and models are shown in Appendix C. We also target randomly initialized LLMs as baselines, given the assertion that SAEs can even interpret randomly initialized Transformers. In our main experiments, we set  $k = 10$  for the TopK FF-KV, and we additionally compare results under varying  $k$  values.

**SAEs.** We use pretrained SAEs from Gemma Scope [30] (width 16k) for Gemma-2-2B and Gemma-2-9B, Llama Scope [21] (width 32k) for Llama-3.1-8B, and SAELens [7] for GPT-2. All SAEs are trained on FF outputs.

<sup>4</sup>It is also marked at which token in the text the feature was activated.

<sup>5</sup>We found SCR and TPP scores are highly unstable, and one may have to treat them as supplementary results. See Appendix B for details.

Model	SAE Type	Coder Status		Concept Detection	
		Feat. Alive $\uparrow$	Expl. Var. $\uparrow$	Absorption $\downarrow$	Sparse Prob. $\uparrow$
Gemma-2 2B	SAE	0.988 $\pm$ 0.000	0.699 $\pm$ 0.000	0.087 $\pm$ 0.173	0.846 $\pm$ 0.161
	Transcoder	1.000 $\pm$ 0.000	0.637 $\pm$ 0.000	0.025 $\pm$ 0.116	0.854 $\pm$ 0.149
	FF-KV	0.999 $\pm$ 0.000	1.000 $\pm$ 0.000	0.000 $\pm$ 0.001	0.827 $\pm$ 0.158
	FF-KV (Norm.)	1.000 $\pm$ 0.000	1.000 $\pm$ 0.000	0.000 $\pm$ 0.001	0.826 $\pm$ 0.160
	TopK-FF-KV	0.984 $\pm$ 0.000	0.160 $\pm$ 0.000	0.000 $\pm$ 0.001	0.768 $\pm$ 0.168
	TopK-FF-KV (Norm.)	0.984 $\pm$ 0.000	0.160 $\pm$ 0.000	0.000 $\pm$ 0.000	0.768 $\pm$ 0.168
	Random Transformer	1.000 $\pm$ 0.000	1.000 $\pm$ 0.000	0.007 $\pm$ 0.013	0.798 $\pm$ 0.067
Llama-3.1 8B	SAE	1.000 $\pm$ 0.000	0.594 $\pm$ 0.000	0.097 $\pm$ 0.332	0.879 $\pm$ 0.123
	Transcoder	-	-	-	-
	FF-KV	1.000 $\pm$ 0.000	1.000 $\pm$ 0.000	0.000 $\pm$ 0.001	0.876 $\pm$ 0.098
	FF-KV (Norm.)	1.000 $\pm$ 0.000	1.000 $\pm$ 0.000	0.000 $\pm$ 0.000	0.876 $\pm$ 0.098
	TopK-FF-KV	0.992 $\pm$ 0.000	0.238 $\pm$ 0.000	0.000 $\pm$ 0.001	0.832 $\pm$ 0.150
	TopK-FF-KV (Norm.)	0.992 $\pm$ 0.000	0.238 $\pm$ 0.000	0.000 $\pm$ 0.001	0.832 $\pm$ 0.150
	Random Transformer	1.000 $\pm$ 0.000	1.000 $\pm$ 0.000	0.002 $\pm$ 0.006	0.837 $\pm$ 0.084

Model	SAE Type	Feature Explanation		Feature Disentanglement	
		Autointerp $\uparrow$	RAVEL-ISO $\uparrow$	RAVEL-CAU $\downarrow$	SCR (k=20) $\uparrow$
Gemma-2 2B	SAE	0.782 $\pm$ 0.274	0.985 $\pm$ 0.027	0.002 $\pm$ 0.006	0.170 $\pm$ 0.191
	Transcoder	0.790 $\pm$ 0.270	0.940 $\pm$ 0.040	0.010 $\pm$ 0.017	0.104 $\pm$ 0.178
	FF-KV	0.710 $\pm$ 0.246	0.952 $\pm$ 0.035	0.012 $\pm$ 0.021	0.041 $\pm$ 0.094
	FF-KV (Norm.)	0.706 $\pm$ 0.255	0.952 $\pm$ 0.035	0.012 $\pm$ 0.021	0.041 $\pm$ 0.120
	TopK-FF-KV	0.772 $\pm$ 0.276	0.943 $\pm$ 0.039	0.009 $\pm$ 0.015	0.045 $\pm$ 0.105
	TopK-FF-KV (Norm.)	0.773 $\pm$ 0.269	0.942 $\pm$ 0.038	0.009 $\pm$ 0.014	0.029 $\pm$ 0.134
	Random Transformer	0.679 $\pm$ 0.248	-	-	0.004 $\pm$ 0.022
Llama-3.1 8B	SAE	0.817 $\pm$ 0.272	0.993 $\pm$ 0.016	0.002 $\pm$ 0.007	0.219 $\pm$ 0.323
	Transcoder	-	-	-	-
	FF-KV	0.751 $\pm$ 0.248	0.955 $\pm$ 0.044	0.007 $\pm$ 0.012	0.048 $\pm$ 0.070
	FF-KV (Norm.)	0.749 $\pm$ 0.245	0.954 $\pm$ 0.044	0.007 $\pm$ 0.012	0.046 $\pm$ 0.071
	TopK-FF-KV	0.807 $\pm$ 0.267	0.954 $\pm$ 0.044	0.006 $\pm$ 0.011	0.030 $\pm$ 0.045
	TopK-FF-KV (Norm.)	0.807 $\pm$ 0.256	0.955 $\pm$ 0.043	0.006 $\pm$ 0.010	0.029 $\pm$ 0.043
	Random Transformer	0.656 $\pm$ 0.237	-	-	0.053 $\pm$ 0.239

Table 1: Overview of the SAE BENCH evaluation results for the middle layer of Gemma-2-2B (layer 13) and Llama-3.1-8B (layer 16). Results are reported as mean  $\pm$  2 standard errors of the mean over multiple seeds/settings. Norm. represent the normalized FF-KV. We also present the scores for a randomly initialized FF layers, which serve as the baseline. No substantial difference between FF-KV and SAEs is observed.

**Transcoders.** We use pretrained Transcoders (TCs) from Gemma Scope [30] for Gemma-2-2B and one from the original paper [12] for GPT-2, respectively.<sup>6</sup>

### 4.3 Results

**Overall.** Table 1 shows the results for each interpretability method. First of all, the SAE-based results and FF-KV results rendered similar tendencies. In each metric, the absolute difference between the scores from different methods is typically much smaller than seed/layer variance. In addition, the difficulty of each task (metric) is aligned across the tasks; for example, SAEs and FF-KVs achieved higher RAVEL-Isolation scores than RAVEL-Causality scores. These results suggest that, even with the activations in the original FF module, comparable interpretability can be realized compared to proxy-based methods, i.e., SAEs and Transcoders.

<sup>6</sup>See Appendix D for more details on the SAEs and Transcoders we use.

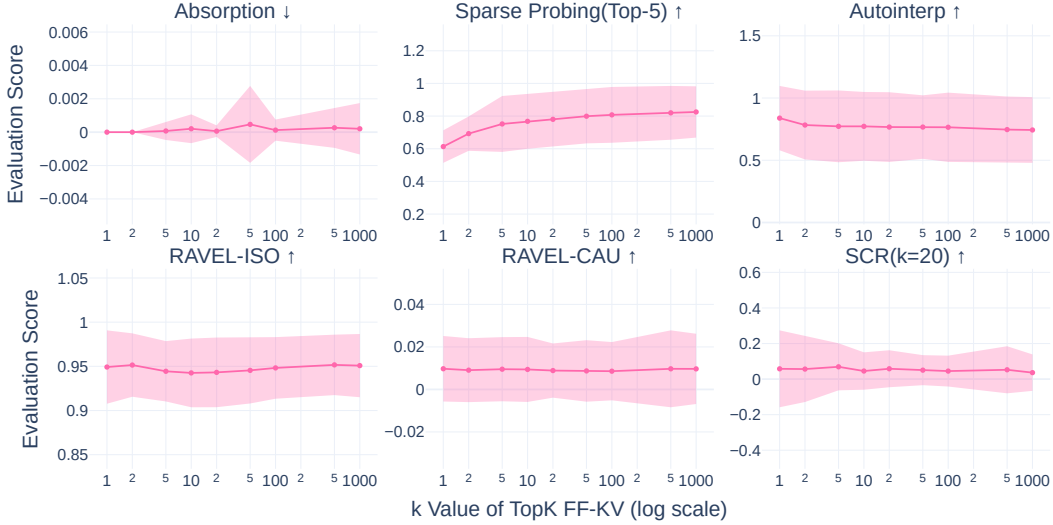


Figure 1: Evaluation scores for TopK FF-KVs at Layer 13 on Gemma-2-2B, under a different sparsity value  $k$ . A higher  $k$  indicates a higher sparsity. Shaded areas denote  $\pm 2$  standard errors of the mean, computed across multiple seeds and evaluation settings.

**Inter-Methods Similarity.** To mention specific similarity among the methods, causal intervention (RAVEL-Causality) was difficult for both SAEs and FF-KVs; that is, FF-KV methods inherit the limitation of SAEs. In contrast, feature isolation is well realized in FF-KVs, similarly to SAEs, even without any specific feature disentanglement regulation in FF-KVs, based on the high scores in RAVEL-isolation. Later layers tend to yield a high RAVEL-isolation score, and vice versa, especially in the case of FF-KVs. This shows a parallel with the existing observation that FFs in later layers have more semantic features [17], and attributes targeted in the RAVEL dataset might not be well-shaped in earlier layers.

**Inter-Methods Difference.** To highlight the differences among the methods, FF-KV methods can achieve perfect explained variance by definition (i.e., zero reconstruction loss as the original model is directly analyzed), whereas SAEs cannot. In addition, FF-KVs exhibited better absorption scores; that is, a simple single concept is not overly split into multiple concepts in FF-KVs than in SAEs, and in this sense, features in FF-KVs are less redundant. Sparse-probing results are comparable or slightly better in FF-KVs; representative features are encoded and generalizable to the same extent in both SAEs and FF-KVs. SAEs achieved slightly but consistently better Auto-interpretability and SCP (although around zero) scores, which are only the advantage of SAEs compared to FF-KV-based analyses.

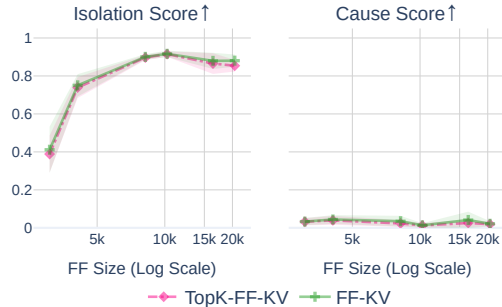


Figure 2: Relationship between FF hidden dimension size (model scale) and RAVEL scores.

**FF-KV Variants.** Within the FF-KV variants, TopK and normalization effects were generally small. Vanilla FF-KV features already exhibited a reasonable interpretability.

**TopK Effects.** Figure 1 shows the relationship between the  $k$  value of the TopK FF-KV (x-axis) and the SAEBENCH evaluation scores (y-axis). The increase of sparsity level leads to inconsistent results, for example, a higher sparse probing (top-5) score but a lower autointerpretation score, suggesting that higher sparsity is not always better, at least for interpretation FF-KV.

**FF-Scaling Effects.** Figure 2 shows the relationship between FF hidden representation size (model scale; x-axis) and RAEL interpretability scores (y-axis). These results suggest that FFs with a larger hidden dimension size do not always get better interpretability results, suggesting that just extending the hidden dimension size of FFs into that of SAEs does not lead to better interpretability. See Appendix E for other metrics.

## 5 Experiment 2: Human Evaluation

Our results in Section 4 suggest that FFs’ internal activations have overall comparable interpretability to SAEs/Transcoders based on automatic evaluations. In this section, we further perform a follow-up manual inspection on the interpretability of features extracted from layer 13 of Gemma-2-2B’s FF-KV, SAE, and Transcoder. We specifically explore the following questions: 1) Do features from the FF-KV, SAE, and Transcoder appear equally interpretable to humans? 2) How accurately can humans infer the origin of the feature?

### 5.1 Settings

We randomly sampled 50 features each from the FF-KV, TopK FF-KV, SAE, and Transcoder of Gemma-2-2B model, yielding a total of 200 features. Each feature  $f_p$  is presented with its top-ten associated texts  $\in \mathcal{S}_p$  based on the activation magnitude over a subset of OpenWebText corpus [19] (200M tokens in total). From the annotator’s view, the presentation order of features is randomly shuffled, and their origins remain hidden throughout the experiment. The annotations in this section were conducted by one of the authors.

Table 2: Number of superficial, conceptual, and uninterpretable features.

Coder	Superficial	Conceptual	Uninterp.
FF-KV	6	8	36
K-FF-KV	9	9	32
SAE	6	9	35
TC	16	11	23

**Interpretability Evaluation.** One annotator judges the qualitative quality of a feature using three categories: 1) *superficial Feature*: activates on shallow surface patterns (e.g., particular word, such as “the,” punctuation, digits); 2) *Conceptual Feature*: activates on higher-level concepts spanning multiple tokens (e.g., sentiment, topics); or, 3) *Uninterpretable*: exhibits no clear activation pattern<sup>7</sup>.

**Feature Origin Judgment.** We also designed a task to predict from which module a feature originates, only based on the feature activation patterns in 10 texts, with the same data, to exploratorily find any difference between these activation patterns. If annotators can not guess which module is used to obtain the given feature, the used methods would have the same level of feature extraction ability. One annotator conducted this analysis, and as preliminary training, the annotator had first learned several activation patterns in the held-out set, paired with their module names.

Table 3: Origin judgment accuracies of features.

Origin	Judging Acc.
FF-KV	0.86
K-FF-KV	0.28
SAE	0.13
TC	0.18

### 5.2 Results

**Interpretability Evaluation.** The results are presented in Table 2. First, the number of conceptual features is nearly the same across the four interpretability methods. In this sense, the quality of the obtained features is comparable. Transcoders could find a larger number of features that are interpretable (superficial or conceptual), but the ratio of superficial features is higher than in the other methods.

**Feature Origin Judgment.** Table 3 shows the results. The annotator could not correctly predict the original model, except for the FF-KV methods. Through interviewing the annotator, we found that they could identify the FF-KV features by relying on superficial patterns in the magnitude and variance of feature activations (FF-KV tends to have a small value with high variance), rather than the represented concepts. Using TopK FF-KV (K-FF-KV) alleviates this distinction pattern, and thus,

<sup>7</sup>We provide the actual text we use to annotate in Appendix F.

if one wants to render a visualization of activations similar to that of SAEs, TopK FF-KV should be preferred. The low accuracies for K-FF-KV, SAE, and TC support that their discovered features and activations are similar to each other, as the human evaluator could not distinguish them.

## 6 Analysis: Feature Alignments

We analyze how similar features discovered by proxy methods, e.g., SAEs, are to the FF-KV ones.

### 6.1 Settings

To investigate the alignment of features from different interpretability methods, we specifically focus on those from FF-KV and Transcoder (not SAE, as the closest counterpart to FF-KV). In this analysis, we used layer 13 of Gemma-2-2B, which showed reasonable performance in the automatic evaluation experiment. Given an  $r$ -th feature vector in the FF  $\mathbf{W}_{V[:,r]}$ , we find the index  $u$  of the most aligned feature vector in  $\mathbf{W}_{\text{dec}}$  from Transcoder, based on their cosine similarity:  $u = \arg \max_k (\mathbf{W}_{V[:,r]} \cdot \mathbf{W}_{\text{dec}[:,k]})$ . Note that when analyzing features in TC, the searching direction will be opposite:  $\arg \max_k (\mathbf{W}_{\text{dec}[:,r]} \cdot \mathbf{W}_{V[:,k]})$ . We call these max-cosine scores MCS.

We first perform a quick check of the correlation between MCS and the semantic feature alignment. For each MCS bin, we sampled ten feature pairs. Then, for feature pairs  $(f_{p_1}, f_{p_2})$  within a specific MCS range, annotators manually inspected their alignment. Similarly to the previous experiment, each feature  $f_p$  is accompanied by ten associated texts  $\in \mathcal{S}_p$  from a subset of the OpenWebText corpus [19]. We consider a pair *matched* if these three criteria meet: 1) The two features generally represent the same concept (e.g., sentiment, topic); OR 2) The associated texts for the two features  $(\mathcal{S}_{p_1}, \mathcal{S}_{p_2})$  exhibits 8/10 overlap; OR 3) The topics of the texts from two features coincide. The annotations in this section were independently conducted by a different author from that of § 5.

### 6.2 Results

**Validity of Cosine-Based Alignments.** The results of alignment analysis are shown in Figure 3. This clearly shows that higher cosine similarity entails their semantic alignment. Based on these results, we tentatively regard a feature pair with cosine similarity above 0.9 as *aligned*, and the similarity below 0.3 as *unaligned* in the following analyses<sup>8</sup>.

#### Large Number of Unaligned Features.

Based on the above criteria with cosine similarity, 41% (=3,780/9,216) and 66% (=10,835/16,384) features in FF-KV and Transcoder are unaligned with each other, respectively. In contrast, 5.7% (=527/9,216) and 3.2% (=527/16,384) features are regarded as aligned in FF-KV and Transcoder, respectively. That is, there are a large number of unaligned features between FF and Transcoder, clarifying that the same level of interpretability from different methods in automatic evaluation (§ 4) was not simply due to their similar feature sets. In the next paragraph, we manually analyze the unaligned features.

#### Feature Complementarity.

We manually analyze three sets of features: (a) aligned features (FF-KV $\cap$ Transcoder), (b) FF-KV features not aligned with any Transcoder feature (FF-KV $\setminus$ Transcoder), and (c) Transcoder features not aligned with any FF-KV feature (Transcoder $\setminus$ FF-KV). The analysis target is the same as § 5; the features are classified into three categories of superficial, conceptual, and uninterpretable. Table 4 shows the distribution of feature categories in each feature set. First and interestingly, the unaligned features both in FFs and TC have a fair amount of conceptual ones. In particular, 28% of features that are unaligned with FFs were conceptual.

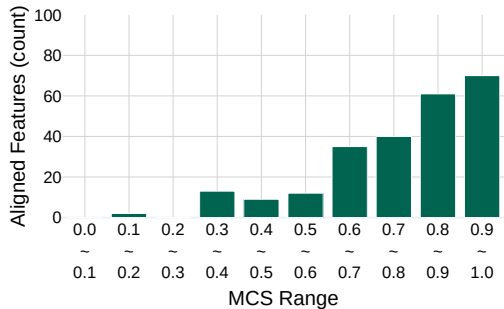


Figure 3: Histogram of aligned features numbers distribution for each MCS bin, between the FF and Transcoder.

<sup>8</sup>See Appendix F for examples of the feature pairs we use for annotation as well as how we decide the threshold.

**Discussion.** Why are there so many unaligned features? One optimistic view is that TC successfully decomposed FF features into simpler ones, resulting in decomposed features being orthogonal to the original FF features, although this may offer a potential side effect of feature absorption, which is suggested by relatively large number of superficial features in  $TC \setminus FF\text{-KV}$  and an already good absorption scores achieved by  $FF\text{-KV}$ s (Table 1). One more pessimistic view is that Transcoder invented completely new features that are not in the original  $FF\text{-KV}$ , which is in line with the fact that SAE can interpret even randomly initialized Transformers [22]. Our analysis alone can not fully distinguish between the two cases, but this fact of frequent misalignment deserves a motivation to further explore the faithfulness of the learned features in proxy modules. Features in the  $FF\text{-KV}$ s will serve as grounding points to evaluate such faithful evaluation, on top of our first extensive attention to  $FF\text{-KV}$ s in the context of SAE research.

Table 4: Number of superficial, multi-token conceptual, and uninterpretable features in aligned/unaligned features between  $FF$  ( $FF\text{-KV}$ ) and Transcoders ( $TC$ ).

Coder	Superficial	Concept.	Uninterp.
$FF\text{-KV} \cap TC$	7	16	27
$FF\text{-KV} \setminus TC$	1	8	41
$TC \setminus FF\text{-KV}$	6	14	23

## 7 Conclusion

In this work, we revisit the interpretability of feature vectors *already represented* in the feed-forward ( $FF$ ) module, as a strong baseline to SAEs. Our results show that the original  $FF$  feature vectors already exhibit reasonable interpretability comparable to that of sparse autoencoders (SAEs) and Transcoders on both comprehensive benchmark and human evaluations. We further demonstrate that a large portion of the features between the  $FF$  and the Transcoder are not aligned, and manual analysis suggests a potential feature over-splitting or hallucination of new features in the proxy module. To sum up, our results demonstrate that SAEs and Transcoders offer only limited advantages over the direct analysis of feed-forward key-value ( $FF\text{-KV}$ ) representations. This finding highlights the lack of a strong and simple baseline within the interpretability community and underscores the importance of including  $FF\text{-KV}$  analysis as a fundamental reference point for evaluating interpretability methods. It also encourages future work to consider both model-internal parameters and proxy-module parameters when pursuing feature-discovery-based interpretability of large language models.

**Limitations.** The feature dimension of SAEs and Transcoders we used was fixed; more diverse configurations should be examined in the comparison, although publicly available pre-trained SAEs/Transcoders are limited, and prior work shows that simply scaling width does not necessarily improve SAEs and that there is not a universally best architecture choice [27]. Not all models are accompanied by Transcoder results: still, training Transcoders on all layers of, e.g., 9B-parameter models is prohibitively costly under an academic budget. We conducted only a few qualitative case studies on the effect of  $k$  for TopK  $FF\text{-KV}$ s and on  $FF$  size. Although our analysis showed a discrepancy between  $FF\text{-KV}$  and Transcoder features, the interpretation of this difference (faithfulness of the learned features) remains unclear; future work should elaborate on this point.

**Impact Statement.** Our findings indicate that SAEs and Transcoders do not consistently outperform the original feature vectors in  $FF$ s with respect to interpretability. We underscore the need to reassess both the interpretability and, potentially, the reproducibility of the previously reported advantages of SAEs. In a sense, our study supports the use of inherently black-box neural LLMs while setting aside the interpretability issue, as their  $FF$ s appear to possess a certain degree of interpretability. Nevertheless, one of the ultimate objectives of this line of research should remain the development of models that are interpretable by design.

**Ethics Statement.** Our research primarily relied on publicly available models and datasets, and strictly adhered to their respective licenses (see Table 7). For human evaluation, we collected data as described in § 5.1. The data were collected with participant consent, and we ensured that responses were anonymized to prevent them from being traced back to individuals. To promote transparency and reproducibility, we have made the collected data, along with all code used in our experiments, publicly accessible. Comprehensive details of our experimental setup are provided in each section and the appendix to ensure reproducibility.

## Acknowledgment

**Author Contribution.** M. Ye led the research project, implemented the experimental pipeline, conducted the SAEBENCH evaluation, designed the human evaluation task, and carried out one of the human evaluation studies. T. Kuribayashi initially proposed the idea of comparing the transcoder with FF-KV augmented by a TopK activation function and was deeply involved in regular discussions throughout the project. T. Inaba provided valuable feedback on implementation, conducted one of the human evaluation studies, and actively contributed to project discussions. J. Suzuki provided overarching guidance and feedback at all stages of the project as well as computational resources.

M. Ye drafted the initial version of the manuscript. T. Kuribayashi offered extensive feedback and revisions on the writing. T. Inaba authored the impact and ethics statements. J. Suzuki contributed valuable insights into the overall framing and positioning of the paper.

**Acknowledgments.** We want to express our gratitude to the members of the Tohoku NLP Group for their insightful comments. And special thanks to Charles Spencer James for assisting in determining the MCS threshold for text alignment through human annotation. This work was supported by the JSPS KAKENHI Grant Number JP24H00727, JP25KJ06300; JST Moonshot R&D Grant Number JPMJMS2011-35 (fundamental research); JST BOOST, Japan Grant Number JPMJBS2421.

## References

- [1] Anthropic. The claude 3 model family: Opus, sonnet, haiku. *arXiv preprint arXiv:2303.08774*, 2024.
- [2] O. Antverg and Y. Belinkov. On the pitfalls of analyzing individual neurons in language models. In *The Tenth International Conference on Learning Representations*, 2022.
- [3] S. Arora, Y. Li, Y. Liang, T. Ma, and A. Risteski. Linear algebraic structure of word senses, with applications to polysemy. *Transactions of the Association for Computational Linguistics*, 6:483–495, 2018.
- [4] S. Biderman, H. Schoelkopf, Q. G. Anthony, H. Bradley, K. O’Brien, E. Hallahan, M. A. Khan, S. Purohit, U. S. Prashanth, E. Raff, A. Skowron, L. Sutawika, and O. Van Der Wal. Pythia: A suite for analyzing large language models across training and scaling. In *Proceedings of the 40th International Conference on Machine Learning*, pages 2397–2430. PMLR, 2023.
- [5] S. Bills, N. Cammarata, D. Mossing, H. Tillman, L. Gao, G. Goh, I. Sutskever, J. Leike, J. Wu, and W. Saunders. Language models can explain neurons in language models, 2023. URL <https://openaipublic.blob.core.windows.net/neuron-explainer/paper/index.html>.
- [6] J. Bloom. Gpt2-small-oai-v5-32k-mlp-out-saes, 2024. URL <https://huggingface.co/jbloom/GPT2-Small-OAI-v5-32k-mlp-out-SAEs>.
- [7] J. Bloom, C. Tigges, A. Duong, and D. Chanin. Saelens, 2024. URL <https://github.com/jbloomAus/SAELens>.
- [8] T. Bricken, A. Templeton, J. Batson, B. Chen, A. Jermyn, T. Conerly, N. Turner, C. Anil, C. Denison, A. Askell, R. Lasenby, Y. Wu, S. Kravec, N. Schiefer, T. Maxwell, N. Joseph, Z. Hatfield-Dodds, A. Tamkin, K. Nguyen, B. McLean, J. E. Burke, T. Hume, S. Carter, T. Henighan, and C. Olah. Towards monosemanticity: Decomposing language models with dictionary learning. *Transformer Circuits Thread*, 2023. URL <https://transformer-circuits.pub/2023/monosemantic-features/index.html>.
- [9] T. Bricken, J. Marcus, S. Mishra-Sharma, M. Tong, E. Perez, M. Sharma, K. Rivoire, T. Henighan, and A. Jermyn. Using dictionary learning features as classifiers. *Transformer Circuits Thread*, 2024. URL <https://transformer-circuits.pub/2024/features-as-classifiers/index.html>.
- [10] T. Brown, B. Mann, N. Ryder, M. Subbiah, J. D. Kaplan, P. Dhariwal, A. Neelakantan, P. Shyam, G. Sastry, A. Askell, S. Agarwal, A. Herbert-Voss, G. Krueger, T. Henighan, R. Child, A. Ramesh, D. Ziegler, J. Wu, C. Winter, C. Hesse, M. Chen, E. Sigler, M. Litwin, S. Gray, B. Chess, J. Clark, C. Berner, S. McCandlish, A. Radford, I. Sutskever, and D. Amodei. Language models are few-shot learners. In *Advances in Neural Information Processing Systems*, volume 33, pages 1877–1901, 2020.

- [11] D. Chanin, J. Wilken-Smith, T. Dulka, H. Bhatnagar, and J. Bloom. A is for absorption: Studying feature splitting and absorption in sparse autoencoders. *arXiv preprint arXiv:2409.14507*, 2024.
- [12] J. Dunefsky, P. Chlenski, and N. Nanda. Transcoders find interpretable llm feature circuits. In *Advances in Neural Information Processing Systems*, volume 37, pages 24375–24410, 2024.
- [13] N. Durrani, H. Sajjad, F. Dalvi, and Y. Belinkov. Analyzing individual neurons in pre-trained language models. In *Proceedings of the 2020 Conference on Empirical Methods in Natural Language Processing*, pages 4865–4880. Association for Computational Linguistics, 2020.
- [14] N. Elhage, T. Hume, C. Olsson, N. Nanda, T. Henighan, S. Johnston, S. ElShowk, N. Joseph, N. DasSarma, B. Mann, D. Hernandez, A. Askell, K. Ndousse, A. Jones, D. Drain, A. Chen, Y. Bai, D. Ganguli, L. Lovitt, Z. Hatfield-Dodds, J. Kernion, T. Conerly, S. Kravec, S. Fort, S. Kadavath, J. Jacobson, E. Tran-Johnson, J. Kaplan, J. Clark, T. Brown, S. McCandlish, D. Amodei, and C. Olah. Softmax linear units. *Transformer Circuits Thread*, 2022. URL <https://transformer-circuits.pub/2022/solu/index.html>.
- [15] L. Gao, S. Biderman, S. Black, L. Golding, T. Hoppe, C. Foster, J. Phang, H. He, A. Thite, N. Nabeshima, S. Presser, and C. Leahy. The pile: An 800gb dataset of diverse text for language modeling. *arXiv preprint arXiv:2101.00027*, 2020.
- [16] L. Gao, T. D. la Tour, H. Tillman, G. Goh, R. Troll, A. Radford, I. Sutskever, J. Leike, and J. Wu. Scaling and evaluating sparse autoencoders. In *The Thirteenth International Conference on Learning Representations*, 2025.
- [17] M. Geva, R. Schuster, J. Berant, and O. Levy. Transformer feed-forward layers are key-value memories. In *Proceedings of the 2021 Conference on Empirical Methods in Natural Language Processing*, pages 5484–5495. Association for Computational Linguistics, 2021.
- [18] M. Geva, A. Caciularu, K. Wang, and Y. Goldberg. Transformer feed-forward layers build predictions by promoting concepts in the vocabulary space. In *Proceedings of the 2022 Conference on Empirical Methods in Natural Language Processing*, pages 30–45. Association for Computational Linguistics, 2022.
- [19] A. Gokaslan and V. Cohen. Openwebtext corpus, 2019. URL <http://SkyLion007.github.io/OpenWebTextCorpus>.
- [20] W. Gurnee, N. Nanda, M. Pauly, K. Harvey, D. Troitskii, and D. Bertsimas. Finding neurons in a haystack: Case studies with sparse probing. *Transactions on Machine Learning Research*, 2023. ISSN 2835-8856.
- [21] Z. He, W. Shu, X. Ge, L. Chen, J. Wang, Y. Zhou, F. Liu, Q. Guo, X. Huang, Z. Wu, Y.-G. Jiang, and X. Qiu. Llama scope: Extracting millions of features from llama-3.1-8b with sparse autoencoders. *arXiv preprint arXiv:2410.20526*, 2024.
- [22] T. Heap, T. Lawson, L. Farnik, and L. Aitchison. Sparse autoencoders can interpret randomly initialized transformers. *arXiv preprint arXiv:2501.17727*, 2025.
- [23] J. Huang, Z. Wu, C. Potts, M. Geva, and A. Geiger. RAVEL: Evaluating interpretability methods on disentangling language model representations. In *Proceedings of the 62nd Annual Meeting of the Association for Computational Linguistics (Volume 1: Long Papers)*, pages 8669–8687. Association for Computational Linguistics, 2024.
- [24] R. Huben, H. Cunningham, L. R. Smith, A. Ewart, and L. Sharkey. Sparse autoencoders find highly interpretable features in language models. In *The Twelfth International Conference on Learning Representations*, 2024.
- [25] T. Inaba, G. Kamoda, K. Inui, M. Isonuma, Y. Miyao, Y. Oseki, B. Heinzerling, and Y. Takagi. How a bilingual lm becomes bilingual: Tracing internal representations with sparse autoencoders. *arXiv preprint arXiv:2503.06394*, 2025.
- [26] S. Kantamneni, J. Engels, S. Rajamanoharan, M. Tegmark, and N. Nanda. Are sparse autoencoders useful? a case study in sparse probing. In *Forty-second International Conference on Machine Learning*, 2025.
- [27] A. Karvonen, C. Rager, J. Lin, C. Tigges, J. I. Bloom, D. Chanin, Y.-T. Lau, E. Farrell, C. S. McDougall, K. Ayonrinde, D. Till, M. Wearden, A. Conmy, S. Marks, and N. Nanda. SAEbench: A comprehensive benchmark for sparse autoencoders in language model interpretability. In *Forty-second International Conference on Machine Learning*, 2025.

- [28] K. Li, O. Patel, F. Viégas, H. Pfister, and M. Wattenberg. Inference-time intervention: Eliciting truthful answers from a language model. In *Advances in Neural Information Processing Systems*, volume 36, pages 41451–41530, 2023.
- [29] Z. Li, C. You, S. Bhojanapalli, D. Li, A. S. Rawat, S. J. Reddi, K. Ye, F. Chern, F. Yu, R. Guo, and S. Kumar. The lazy neuron phenomenon: On emergence of activation sparsity in transformers. In *The Eleventh International Conference on Learning Representations*, 2023.
- [30] T. Lieberum, S. Rajamanoharan, A. Conmy, L. Smith, N. Sonnerat, V. Varma, J. Kramar, A. Dragan, R. Shah, and N. Nanda. Gemma scope: Open sparse autoencoders everywhere all at once on gemma 2. In *Proceedings of the 7th BlackboxNLP Workshop: Analyzing and Interpreting Neural Networks for NLP*, 2024.
- [31] S. Marks and M. Tegmark. The geometry of truth: Emergent linear structure in large language model representations of true/false datasets. In *First Conference on Language Modeling*, 2024.
- [32] S. Marks, C. Rager, E. J. Michaud, Y. Belinkov, D. Bau, and A. Mueller. Sparse feature circuits: Discovering and editing interpretable causal graphs in language models. In *The Thirteenth International Conference on Learning Representations*, 2025.
- [33] N. Nanda and J. Bloom. Transformerlens, 2022. URL <https://github.com/TransformerLensOrg/TransformerLens>.
- [34] C. Olsson, N. Elhage, N. Nanda, N. Joseph, N. DasSarma, T. Henighan, B. Mann, A. Askell, Y. Bai, A. Chen, T. Conerly, D. Drain, D. Ganguli, Z. Hatfield-Dodds, D. Hernandez, S. Johnston, A. Jones, J. Kernion, L. Lovitt, K. Ndousse, D. Amodei, T. Brown, J. Clark, J. Kaplan, S. McCandlish, and C. Olah. In-context learning and induction heads. *arXiv preprint arXiv:2209.11895*, 2022.
- [35] OpenAI. Gpt-4 technical report. *arXiv preprint arXiv:2303.08774*, 2024.
- [36] G. S. Paulo, A. T. Mallen, C. Juang, and N. Belrose. Automatically interpreting millions of features in large language models. In *Forty-second International Conference on Machine Learning*, 2025.
- [37] T. Pimentel, N. Saphra, A. Williams, and R. Cotterell. Pareto probing: Trading off accuracy for complexity. In *Proceedings of the 2020 Conference on Empirical Methods in Natural Language Processing*, pages 3138–3153. Association for Computational Linguistics, 2020.
- [38] T. Pimentel, J. Valvoda, N. Stoehr, and R. Cotterell. The architectural bottleneck principle. In Y. Goldberg, Z. Kozareva, and Y. Zhang, editors, *Proceedings of the 2022 Conference on Empirical Methods in Natural Language Processing*, pages 11459–11472. Association for Computational Linguistics, 2022.
- [39] A. Radford, J. Wu, R. Child, D. Luan, D. Amodei, and I. Sutskever. Language models are unsupervised multitask learners. *OpenAI*, 2019. URL [https://cdn.openai.com/better-language-models/language\\_models\\_are\\_unsupervised\\_multitask\\_learners.pdf](https://cdn.openai.com/better-language-models/language_models_are_unsupervised_multitask_learners.pdf).
- [40] H. Sajjad, N. Durrani, and F. Dalvi. Neuron-level interpretation of deep NLP models: A survey. *Transactions of the Association for Computational Linguistics*, 10:1285–1303, 2022.
- [41] N. Shazeer. Glu variants improve transformer. *arXiv preprint arXiv:2002.05202*, 2020.
- [42] X. Suau, L. Zappella, and N. Apostoloff. Finding experts in transformer models. *arXiv preprint arXiv:2005.07647*, 2020.
- [43] G. Team. Gemma 2: Improving open language models at a practical size. *arXiv preprint arXiv:2408.00118*, 2024.
- [44] G. Team. Gemini: A family of highly capable multimodal models. *arXiv preprint arXiv:2312.11805*, 2024.
- [45] L. Team. The llama 3 herd of models. *arXiv preprint arXiv:2407.21783*, 2024.
- [46] A. Templeton, T. Conerly, J. Marcus, J. Lindsey, T. Bricken, B. Chen, A. Pearce, C. Citro, E. Ameisen, A. Jones, H. Cunningham, N. L. Turner, C. McDougall, M. MacDiarmid, C. D. Freeman, T. R. Sumers, E. Rees, J. Batson, A. Jermyn, S. Carter, C. Olah, and T. Henighan. Scaling monosemanticity: Extracting interpretable features from claude 3 sonnet. *Transformer Circuits Thread*, 2024. URL <https://transformer-circuits.pub/2024/scaling-monosemanticity/index.html>.

- [47] I. Tenney, D. Das, and E. Pavlick. BERT rediscovers the classical NLP pipeline. In *Proceedings of the 57th Annual Meeting of the Association for Computational Linguistics*, pages 4593–4601. Association for Computational Linguistics, 2019.
- [48] C. Tigges. Pythia-70m-deduped-mlp-sm, 2024. URL [https://huggingface.co/ctigges/pythia-70m-deduped\\_\\_mlp-sm\\_processed](https://huggingface.co/ctigges/pythia-70m-deduped__mlp-sm_processed).
- [49] N. L. Turner, A. Jermyn, J. Batson, and J. Batson. Measuring feature sensitivity using dataset filtering. *Transformer Circuits Thread*, 2024. URL <https://transformer-circuits.pub/2024/july-update/index.html#feature-sensitivity>.
- [50] E. Voita and I. Titov. Information-theoretic probing with minimum description length. In B. Webber, T. Cohn, Y. He, and Y. Liu, editors, *Proceedings of the 2020 Conference on Empirical Methods in Natural Language Processing*, pages 183–196. Association for Computational Linguistics, 2020.
- [51] Z. Wu, A. Arora, A. Geiger, Z. Wang, J. Huang, D. Jurafsky, C. D. Manning, and C. Potts. Axbench: Steering LLMs? even simple baselines outperform sparse autoencoders. In *Forty-second International Conference on Machine Learning*, 2025.
- [52] J. Xin, J. Lin, and Y. Yu. What part of the neural network does this? understanding LSTMs by measuring and dissecting neurons. In *Proceedings of the 2019 Conference on Empirical Methods in Natural Language Processing and the 9th International Joint Conference on Natural Language Processing (EMNLP-IJCNLP)*, pages 5823–5830. Association for Computational Linguistics, 2019.
- [53] Z. Yun, Y. Chen, B. Olshausen, and Y. LeCun. Transformer visualization via dictionary learning: contextualized embedding as a linear superposition of transformer factors. In *Proceedings of Deep Learning Inside Out (DeeLIO): The 2nd Workshop on Knowledge Extraction and Integration for Deep Learning Architectures*, pages 1–10. Association for Computational Linguistics, 2021.
- [54] S. Zhong, M. Xu, T. Ao, and G. Shi. Understanding transformer from the perspective of associative memory. *arXiv preprint arXiv:2505.19488*, 2025.

## A Implementation Details on FF-KVs

### A.1 Overall Framework

We implement FF-KVs use the `custom_sae` class provided by SAEBENCH [7]. To faithfully reproduce the activation of the FF sublayers, we apply the hook-based approach. The `encode` method simulates the FF’s forward pass up to its neuron activations. It takes an input tensor  $\mathbf{x}$ , injects it at the FF’s input hook point, and captures the subsequent neuron activations using another hook. Conversely, the `decode` method simulates the FF’s transformation from its neuron activations to its output. It accepts a tensor of neuron activations, injects them at the corresponding hook point, and captures the FF’s final output. A `forward` method is also provided, performing the full pass through the FF block using hooks to inject input and capture the final output. This framework allows for the direct examination of an FF’s feature extraction and signal reconstruction capabilities as if it were an SAE, providing a unique lens for interpreting learned representations within large language models.

### A.2 FF-KV Implement Details

The core principle is to map the FF’s operations to the conceptual stages of an SAE:

**Input.** Activations entering the FF block serve as the input to our pseudo-SAE.

**Feature Representation (Encoding).** The FF’s internal neuron activations, captured after the non-linear activation function and any gating, are interpreted as the SAE’s latent features. The dimensionality of this feature space is equivalent to the FF’s hidden dimension. The effective “encoder weights” are the FF’s input weights.

**Reconstruction (Decoding).** The FF’s output, which is typically added to the residual stream, is considered the reconstructed input. The effective “decoder weights” and “decoder bias” are the FF’s output weights and output bias, respectively.

### A.3 TopK FF-KV Implement Details

The TopK FF-KV extends the FF-KV framework by enforcing a strict TopK sparsity on the intermediate feature representations. The only modification from a FF-KV resides in the `encode` method. After obtaining the FF’s internal neuron activations, a k-sparsity constraint is applied. For each input position (e.g., token in a sequence), the method identifies the  $k$  neuron activations with the largest absolute values. All other neuron activations for that position are set to zero. This results in a feature vector where, at most,  $k$  dimensions are non-zero.

### A.4 Normalized FF-KV Implement Details

The FF block’s original output weights (which serve as the “decoder weights”) are  $L_2$ -normalized along their feature dimension. The original norms of these weight vectors are stored. The `encode` and `forward` methods remain unchanged from their respective base FF-KV implementations. The key difference lies in the `decode` method. Before applying the normalized “decoder weights”, the input feature activations are first scaled by the stored original norms. This step ensures that the magnitude of the reconstructed output appropriately reflects the original scaling of the FF block’s output projections, despite the normalization. For models that include a final normalization step after the FF output (e.g., Gemma-2 Models), this step is also applied to maintain fidelity with the original model’s computation.

### A.5 Transcoder Implement Details

We load the Transcoder weight into the `JumpReLU` class of SAEBENCH. While evaluating it, we follow the instructions of Gemma-Scope paper [30] to load model weights with folding applied.

## B Details on Metrics

We provide detailed definitions of the metrics used in our main results, alongside the experimental settings for each metric.

**Feature Alive Rate.** This metric belongs to the “core” evaluations in SAEBENCH. It counts how many features are alive out of the  $d_{\text{coder}}$  total features. A feature is deemed active when its activation exceeds 0. The evaluation is conducted on a 4 M-token subset of OpenWebText [19].

The metric is especially relevant for TopK FF-KVs employing a TOPK activation, ensuring that the mechanism does not repeatedly select only a small subset of neurons.

**Explained Variance.** Also in the “core” suite, this metric is computed on a 0.4 M-token subset of OpenWebText [19].

**Absorption Score.** Feature absorption [11] stems from *feature splitting* [8, 49], in which newly uncovered features become overly specific. A concrete example is a feature that activates only on “U.S. cities except New York and Los Angeles.”

The metric targets a first-letter classification task, measuring situations where the main feature for a letter fails to fully capture the concept of “first letter”, and other features compensate. Specifically, it evaluates all 26 letters with the prompt “*{word}* has the first letter:”.

Given primary features  $S_{\text{main}}$  (e.g., selected via sparse probing) and auxiliary features  $S_{\text{abs}}$ , the absorption score for one input is

$$\text{Absorption} = \frac{\sum_{i \in S_{\text{abs}}} a_i d_i \cdot p}{\sum_{i \in S_{\text{abs}}} a_i d_i \cdot p + \sum_{i \in S_{\text{main}}} a_i d_i \cdot p},$$

where  $a_i$  is the activation,  $d_i$  the unit decoder direction, and  $p$  the ground-truth probe direction. We use the default hyperparameters.

**Sparse Probing.** Sparse probing, introduced by Gurnee et al. [20], evaluates the alignment between individual features and a prespecified concept  $c$ . It has a hyperparameter  $K$  that specifies how many features are used when training the probe. For each feature  $h_j$ ,

$$s_j = \left| \mathbb{E}_{x \in \mathcal{X}_+} [h_j(x)] - \mathbb{E}_{x \in \mathcal{X}_-} [h_j(x)] \right|, \tag{8}$$

where  $\mathcal{X}_+$  and  $\mathcal{X}_-$  denote inputs with and without  $c$ , respectively. The top  $K$  features by  $s_j$  serve as inputs to a logistic-regression probe; the probe’s test accuracy constitutes the sparse-probing score. We again employ the default hyperparameters.

**Auto-Interpretation Score.** This evaluation has two phases: generation and scoring. In the generation phase, it obtain SAE activations, annotate each token with its activation value for the feature under consideration, and prompt an LLM to generate explanations based on these annotated activation patterns. The scoring phase constructs a test set for each feature containing 14 examples, exactly two of which are activated texts. The LLM must label each of the 14 texts as activated or not; the resulting prediction accuracy yields the auto-interpretation score.

The dataset is a subset of the copyright-free version of the Pile [15] (monology/pile-uncopyrighted), comprising 2 M tokens. GPT-4o [35] is used both to generate explanations and to predict activations.

**SCR and TPP** Following SHIFT [32], the SCR evaluation proceeds as follows. A baseline classifier  $C_{\text{base}}$  is trained on data containing both true and spurious correlations. We then zero-ablate the  $K$  features most attributable to the spurious signal and re-measure accuracy on a balanced set:

$$\text{SCR} = \frac{A_{\text{abl}} - A_{\text{base}}}{A_{\text{oracle}} - A_{\text{base}}},$$

where  $A_{\text{abl}}$  is the post-ablation accuracy,  $A_{\text{base}}$  the baseline accuracy, and  $A_{\text{oracle}}$  the accuracy of an oracle probe trained on the true concept.

**TPP.** We extend Targeted Probe Perturbation to the multi-class setting. For  $m$  classes, let  $C_j$  be a linear probe that classifies concept  $c_j$  with accuracy  $A_j$ . Let  $A_{i,j}$  denote the accuracy of probe  $C_j$  after ablating the  $K$  most contributive features for class  $c_i$ . The TPP score is then

$$\text{TPP} = \frac{1}{m} \sum_{i=1}^m (A_{i,i} - A_i) - \frac{1}{m(m-1)} \sum_{i \neq j} (A_{i,j} - A_j),$$

so higher SCR and TPP values indicate stronger disentanglement.

**Stability Caveats.** Both metrics are highly sensitive to the choice of  $K$ . Across different  $K$  values, SCR can range from below 0.1 to above 0.4. For TPP the variation is even larger: for the same coders, scores span from under 0.1 (SAE,  $K = 2$ , Figure 14) to over 0.4 (SAE,  $K = 50$ , Figure 18). Error bands obtained from multiple sub-runs are also wide—not only for SAEs (e.g., SAE on Llama-3.1 in Figure 14, and on Pythia in Figure 15) but likewise for FF-KVs (e.g., Pythia in Figure 14 and Figure 15).

Based on these empirical observations, we interpret SCR and TPP scores with caution.

**RAVEL.** Unlike SCR and TPP, we find RAVEL to be consistent across multiple models and coders, and the results align with the scores reported in the original work [23]. This stability suggests that RAVEL is comparatively insensitive to hyperparameter choices and dataset splits, making it a reliable baseline when assessing disentanglement. Accordingly, we place greater weight on RAVEL when synthesizing conclusions across metrics.

## C Detailed Results on SAEBENCH

We provide detailed evaluation result with error bars indicate 95% confidence intervals ( $\pm 2$  SEM), compute as  $\text{SEM} = \sqrt{\frac{\sum (x_i - \bar{x})^2}{n(n-1)}}$  where  $n$  is the number of runs on different datasets for each metric in each layer. Note that error bars are not applicable for the feature alive metric, as they are counts for features activated at least once.

### C.1 Detailed Results on More Models

Figures 5, 6, 10, 13, 7, 8, 9, and 17 present the detailed results for all models.

### C.2 Detailed Results on Various Hyperparameter Choices

For metrics that have multiple hyperparameter choices for  $k$ , we provide detailed results for all tested hyperparameters.

- For SCR, the available  $k$  values are 2, 5, 10, 20, 50, 100, and 500; the corresponding results are shown in Figures 14, 15, 16, 17, 18, 19, and 20.
- For TPP, the available  $k$  values are the same, and all results are shown in Figures 21, 22, 23, 24, 25, 26, and 27.
- For Sparse Probing, the available  $k$  values are 1, 2, and 5; the results are shown in Figures 11, 12, and 13.

## D Details on SAEs/Transcoders used

For both SAEs and Transcoders from Gemma-Scope, we use the *canonical* versions, whose average  $L_0$  sparsity is close to 100, which are believed to be reasonably useful<sup>9</sup>. The SAEs are loaded through SAELens [7] with the following keys: “gemma-scope-2b-pt-mlp-canonical” for Gemma-2-2B, “gemma-scope-9b-pt-mlp-canonical” for Gemma-2-9B, and “llama\_scope\_lxm\_8x” for Llama-3.1-8B.

For Transcoders, since no canonical versions have been explicitly defined and the SAELens release we use does not yet support loading them, we manually select checkpoints from the Gemma-Scope

<sup>9</sup>This statement can be found on Gemma Scope’s collection page on HuggingFace (link).

Layer	ID
0	layer_0/width_16k/average_10_115/params.npz
1	layer_1/width_16k/average_10_104/params.npz
2	layer_2/width_16k/average_10_87/params.npz
3	layer_3/width_16k/average_10_96/params.npz
4	layer_4/width_16k/average_10_88/params.npz
5	layer_5/width_16k/average_10_87/params.npz
6	layer_6/width_16k/average_10_95/params.npz
7	layer_7/width_16k/average_10_70/params.npz
8	layer_8/width_16k/average_10_92/params.npz
9	layer_9/width_16k/average_10_72/params.npz
10	layer_10/width_16k/average_10_88/params.npz
11	layer_11/width_16k/average_10_108/params.npz
12	layer_12/width_16k/average_10_111/params.npz
13	layer_13/width_16k/average_10_89/params.npz
14	layer_14/width_16k/average_10_81/params.npz
15	layer_15/width_16k/average_10_78/params.npz
16	layer_16/width_16k/average_10_87/params.npz
17	layer_17/width_16k/average_10_112/params.npz
18	layer_18/width_16k/average_10_99/params.npz
19	layer_19/width_16k/average_10_89/params.npz
20	layer_20/width_16k/average_10_88/params.npz
21	layer_21/width_16k/average_10_102/params.npz
22	layer_22/width_16k/average_10_117/params.npz
23	layer_23/width_16k/average_10_116/params.npz
24	layer_24/width_16k/average_10_96/params.npz
25	layer_25/width_16k/average_10_110/params.npz

Table 5: Mapping of layers to their corresponding IDs

collection and download the corresponding weights from HuggingFace (link). These checkpoints are chosen according to the same criteria as the *canonical* SAEs, and their exact filenames are listed in Table 5. We also directly download the weight from the Transcoder proposal work [12] on HuggingFace (Link). To the best of our knowledge, there are no Transcoders publicly available for Gemma-2-9B and Llama-3.1-8B, and Pythia-70M.

## E Detailed Results on FF Scaling

Table 6 shows the results on all metrics regarding to various FF intermediate sizes. Scores are not showing noticeable improvement except for RAVEL and absorption. Trends shown in SCR somehow understandable: these metrics highly depend on the ground truth probing performance, which is not always stable. Sparse probing result is also understandable, since sparse probing on FF from a random transfer can achieve a reasonable score, the probs can learn unintended signal in the dataset, rather than the true feature.

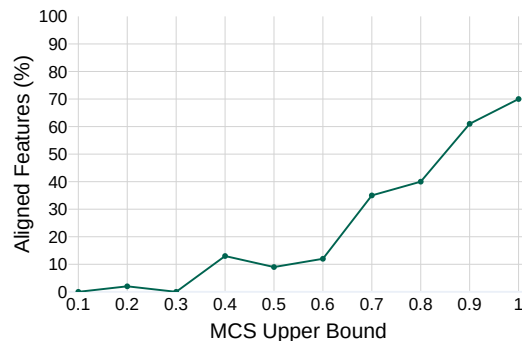


Figure 4: Proportion of aligned features as a function of the max-cosine score (MCS).

## F Feature Examples

We provide example features for each annotation and coder, visualizing the top input examples that most strongly activate each feature. All features are extracted from layer 13 of Gemma-2-2B. To analyze the relationship between alignment and the max-cosine score (MCS), we divide the MCS

Table 6: Evaluation scores for different size of Pythia models’ FF and TopK FF-KVs.

FF Size	SAE Type	Coder Status		Concept Detection	
		Feat. Alive $\uparrow$	Expl. Var. $\uparrow$	Absorption $\downarrow$	Sparse Prob. $\uparrow$
2048	FF-KV	1.000 $\pm$ 0.000	1.000 $\pm$ 0.000	0.060 $\pm$ 0.083	0.802 $\pm$ 0.173
	TopK-FFKV	1.000 $\pm$ 0.000	0.227 $\pm$ 0.000	0.064 $\pm$ 0.127	0.717 $\pm$ 0.204
3072	FF-KV	1.000 $\pm$ 0.000	1.000 $\pm$ 0.000	0.013 $\pm$ 0.038	0.826 $\pm$ 0.140
	TopK-FFKV	0.999 $\pm$ 0.000	0.129 $\pm$ 0.000	0.014 $\pm$ 0.036	0.779 $\pm$ 0.153
4096	FF-KV	1.000 $\pm$ 0.000	1.000 $\pm$ 0.000	0.003 $\pm$ 0.007	0.803 $\pm$ 0.128
	TopK-FFKV	1.000 $\pm$ 0.000	0.082 $\pm$ 0.000	0.006 $\pm$ 0.011	0.765 $\pm$ 0.126
8192	FF-KV	1.000 $\pm$ 0.000	1.000 $\pm$ 0.000	0.003 $\pm$ 0.009	0.812 $\pm$ 0.194
	TopK-FFKV	1.000 $\pm$ 0.000	0.277 $\pm$ 0.000	0.003 $\pm$ 0.009	0.770 $\pm$ 0.186
10240	FF-KV	1.000 $\pm$ 0.000	1.000 $\pm$ 0.000	0.001 $\pm$ 0.004	0.850 $\pm$ 0.117
	TopK-FFKV	1.000 $\pm$ 0.000	0.090 $\pm$ 0.000	0.002 $\pm$ 0.009	0.783 $\pm$ 0.144
16384	FF-KV	1.000 $\pm$ 0.000	1.000 $\pm$ 0.000	0.001 $\pm$ 0.003	0.870 $\pm$ 0.119
	TopK-FFKV	1.000 $\pm$ 0.000	0.047 $\pm$ 0.000	0.001 $\pm$ 0.004	0.807 $\pm$ 0.155
20480	FF-KV	1.000 $\pm$ 0.000	1.000 $\pm$ 0.000	0.002 $\pm$ 0.005	0.818 $\pm$ 0.164
	TopK-FFKV	1.000 $\pm$ 0.000	0.195 $\pm$ 0.000	0.000 $\pm$ 0.001	0.735 $\pm$ 0.157

FF Size	SAE Type	Feature Explanation		Feature Disentanglement	
		Autointerp $\uparrow$	RAVEL-ISO $\uparrow$	RAVEL-CAU $\downarrow$	SCR (k=20) $\uparrow$
2048	FF-KV	0.727 $\pm$ 0.256	-	-	-0.056 $\pm$ 0.464
	TopK-FFKV	0.766 $\pm$ 0.277	-	-	0.000 $\pm$ 0.131
3072	FF-KV	0.734 $\pm$ 0.252	0.411 $\pm$ 0.272	0.033 $\pm$ 0.043	0.093 $\pm$ 0.195
	TopK-FFKV	0.731 $\pm$ 0.271	0.389 $\pm$ 0.218	0.032 $\pm$ 0.043	0.017 $\pm$ 0.114
4096	FF-KV	0.708 $\pm$ 0.252	0.750 $\pm$ 0.132	0.044 $\pm$ 0.051	0.017 $\pm$ 0.054
	TopK-FFKV	0.716 $\pm$ 0.263	0.739 $\pm$ 0.123	0.039 $\pm$ 0.053	-0.001 $\pm$ 0.028
8192	FF-KV	0.714 $\pm$ 0.256	0.900 $\pm$ 0.032	0.035 $\pm$ 0.064	0.047 $\pm$ 0.099
	TopK-FFKV	0.712 $\pm$ 0.271	0.897 $\pm$ 0.031	0.023 $\pm$ 0.040	0.016 $\pm$ 0.038
10240	FF-KV	0.707 $\pm$ 0.259	0.916 $\pm$ 0.037	0.013 $\pm$ 0.025	0.049 $\pm$ 0.130
	TopK-FFKV	0.704 $\pm$ 0.278	0.915 $\pm$ 0.033	0.013 $\pm$ 0.026	-0.017 $\pm$ 0.065
16384	FF-KV	0.702 $\pm$ 0.254	0.879 $\pm$ 0.095	0.041 $\pm$ 0.098	0.023 $\pm$ 0.056
	TopK-FFKV	0.701 $\pm$ 0.265	0.865 $\pm$ 0.122	0.025 $\pm$ 0.046	0.003 $\pm$ 0.018
20480	FF-KV	0.693 $\pm$ 0.252	0.881 $\pm$ 0.072	0.021 $\pm$ 0.031	0.030 $\pm$ 0.050
	TopK-FFKV	0.698 $\pm$ 0.270	0.854 $\pm$ 0.069	0.019 $\pm$ 0.028	0.022 $\pm$ 0.064

range into ten bins (e.g., 0.1–0.2, 0.2–0.3). From each bin, we sample ten features, each associated with ten pairs of input examples (for a total of 100 examples per bin), and annotate the proportion of aligned features within each bin. As shown in Figure 4, features with an MCS below 0.3 are almost never aligned, whereas those above 0.9 exhibit over 60% alignment.

## F.1 Superficial Features

We show examples of “superficial” features here.

- **Figure 29** shows the first FF-KV feature we annotate as superficial, activating on “now”.
- **Figure 30** shows the first TopK FF-KV feature we annotate as superficial, focused on “the”.
- **Figure 31** shows the first SAE feature we annotate as superficial, activating on “return” in code.
- **Figure 32** shows the first Transcoder feature we annotate as superficial, activating on alphanumeric token combinations.

## F.2 Conceptual Features

We illustrate features that activate on higher-level concepts or semantic themes.

- **Figure 33** shows the first FF-KV feature we annotate as conceptual, activating on coastal concepts.
- **Figure 34** shows the first TopK FF-KV feature we annotate as conceptual, linked to recipes and desserts.
- **Figure 35** shows the first SAE feature we annotate as conceptual, activating on country and region names.
- **Figure 36** shows the first Transcoder feature we annotate as conceptual, activating on college degree concepts.

## F.3 Uninterpretable Features

We also show examples of features without clear patterns.

- **Figure 37** shows the first FF-KV feature we annotate as uninterpretable.
- **Figure 38** shows the first TopK FF-KV feature we annotate as uninterpretable.
- **Figure 39** shows the first SAE feature we annotate as uninterpretable.
- **Figure 40** shows the first Transcoder feature we annotate as uninterpretable.

## F.4 Aligned Features

**Figure 41** shows the first FF-KV feature we annotate as uninterpretable.

## F.5 Unaligned Features

**Figure 42** shows the first FF-KV feature we annotate as uninterpretable.

Table 7: The list of assets used in this work.

Asset Type	Asset Name	Link	License	Citation
Code	SAEBench		Not specified	[27]
Code	TransformerLens		MIT License	[33]
Code	SAELens		MIT License	[7]
Dataset	OpenWebText	Link	CC0 1.0 Universal	[19]
SAE	Gemma-Scope-2B-pt-mlp	google/gemma-scope-2b-pt-mlp	Apache 2.0	[30]
SAE	Gemma-Scope-9B-pt-mlp	google/gemma-scope-9b-pt-mlp	Apache 2.0	[30]
SAE	Llama-Scope-3.1-8B-LXM-8x	fnlp/Llama3_1-8B-Base-LXM-8x	Not specified	[21]
SAE	GPT2-Small-32k-mlp-out	jbloom/GPT2-Small-OAI-v5-32k-mlp-out-SAEs	Not specified	[6]
SAE	Pythia-70m-deduped-mlp	ctigges/pythia-70m-deduped__mlp-sm_processed	Not specified	[48]
Transcoder	Gemma-Scope-2B-pt-transcoders	google/gemma-scope-2b-pt-transcoders	Apache 2.0	[30]
Model	GPT-2-small	openai-community/gpt2	MIT License	[39]
Model	Gemma-2-2B	google/gemma-2-2b	Gemma License	[43]
Model	Gemma-2-9B	google/gemma-2-9b	Gemma License	[43]
Model	Llama-3.1-8B	meta-llama/Llama-3.1-8B	Llama 3 Community License	[45]
Model	Pythia-70M-deduped	EleutherAI/pythia-70m-deduped	Apache 2.0	[4]
Model	Pythia-160M-deduped	EleutherAI/pythia-160m-deduped	Apache 2.0	[4]
Model	Pythia-410M-deduped	EleutherAI/pythia-410m-deduped	Apache 2.0	[4]
Model	Pythia-1.4B-deduped	EleutherAI/pythia-1.4b-deduped	Apache 2.0	[4]
Model	Pythia-2.8B-deduped	EleutherAI/pythia-2.8b-deduped	Apache 2.0	[4]
Model	Pythia-6.9B-deduped	EleutherAI/pythia-6.9b-deduped	Apache 2.0	[4]
Model	Pythia-12B-deduped	EleutherAI/pythia-12b-deduped	Apache 2.0	[4]

## G Use of Existing Assets

Table 7 shows the assets being used in this paper, with the type, name, link, license, and citation for each asset used in the paper.

## H Compute Statement

Most experiments presented in this paper were run on a cluster consisting of the NVIDIA H200 GPUs with 141GB of memory. All experiments on models are run using a single 141GB memory GPU. Evaluation time per layer differs largely on model size, with Pythia-70M, it takes approximately 1 hour, and for larger models like Gemma-2-9B, it takes approximately 4 hours per layer. The total GPU time for this work is approximately 1400 hours, including exploratory research stage.

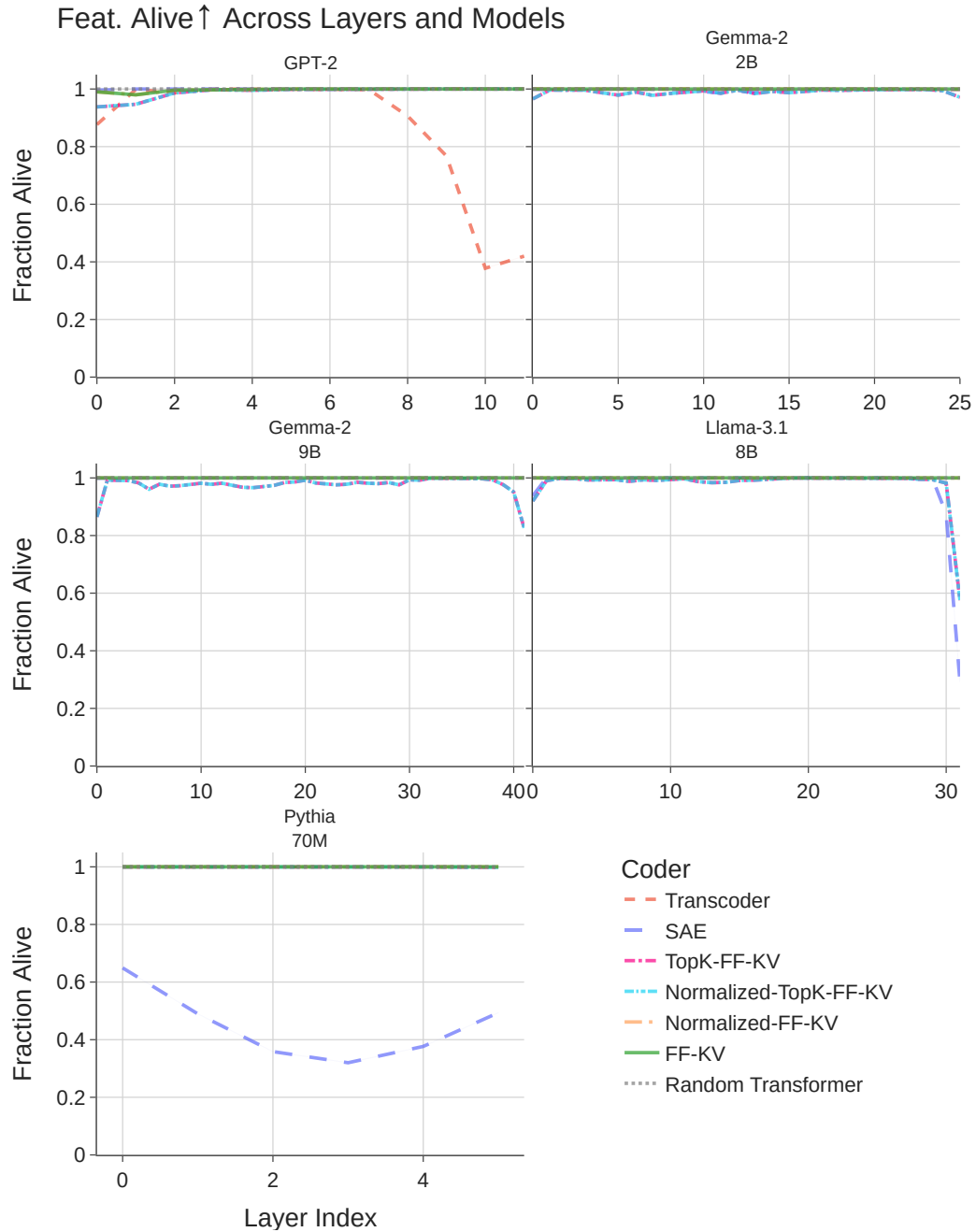


Figure 5: Detailed feature alive scores on all tested models, across all layers.

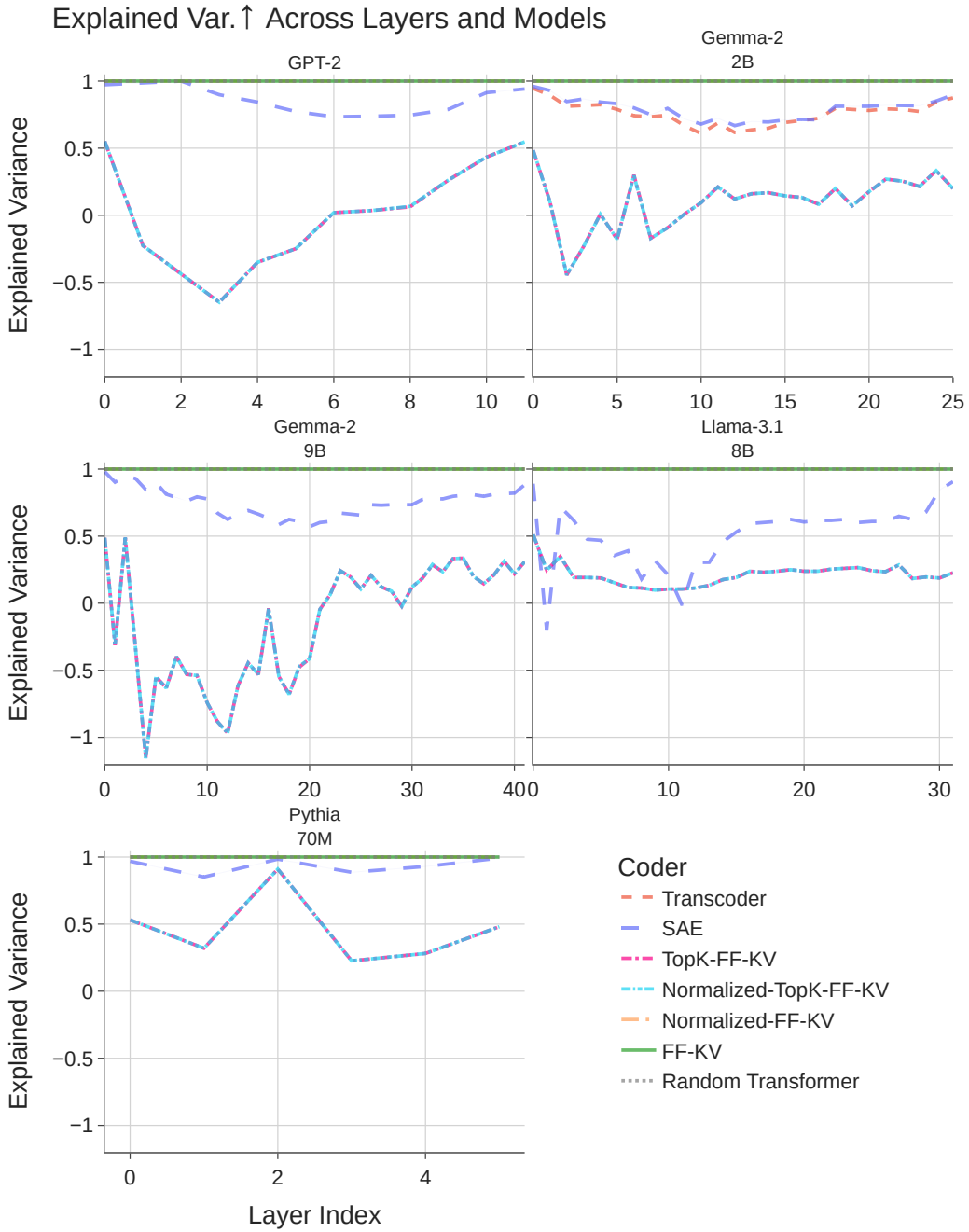


Figure 6: Detailed explained variance scores on all tested models, across all layers.

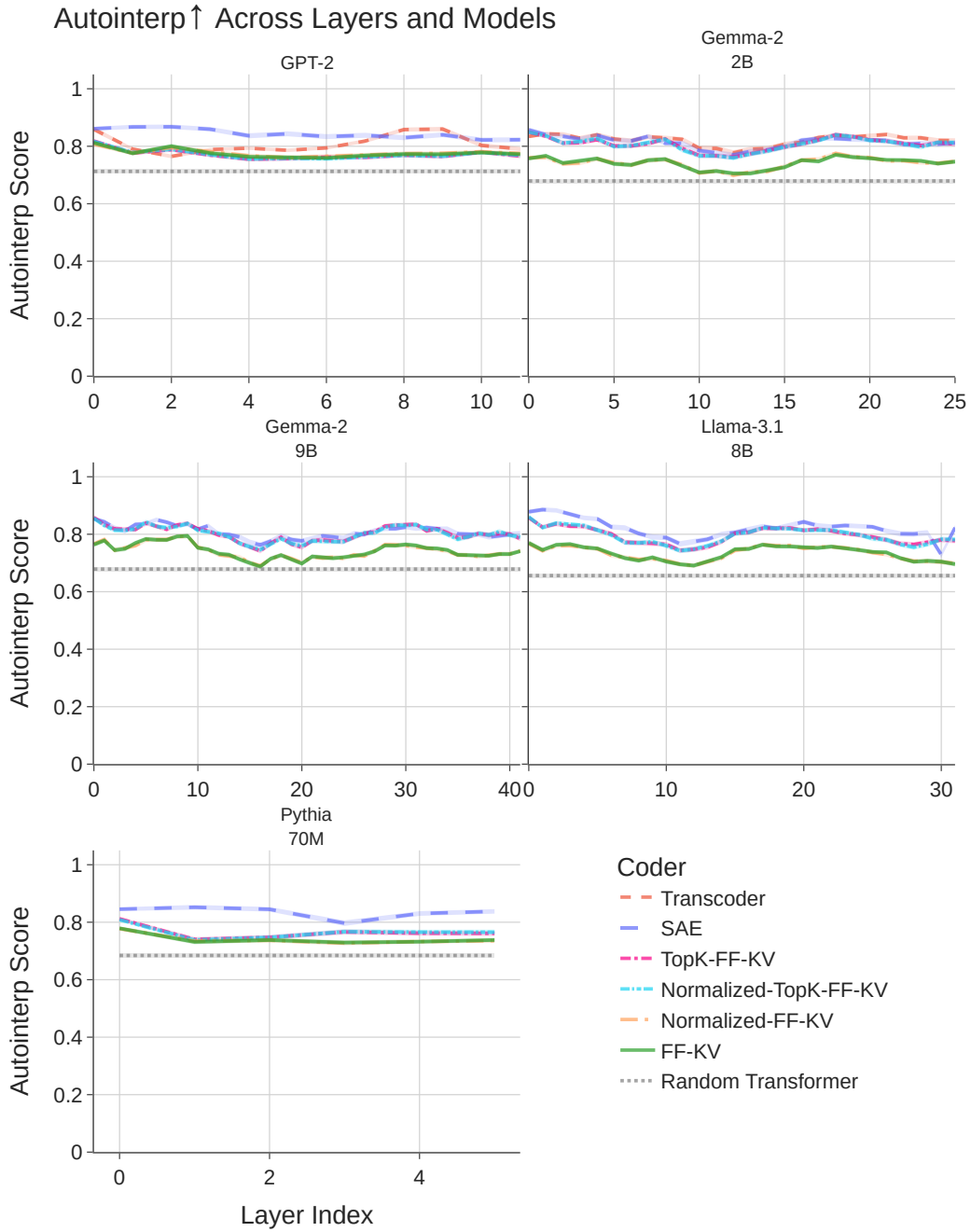


Figure 7: Detailed auto-interpretation scores on all tested models, across all layers.

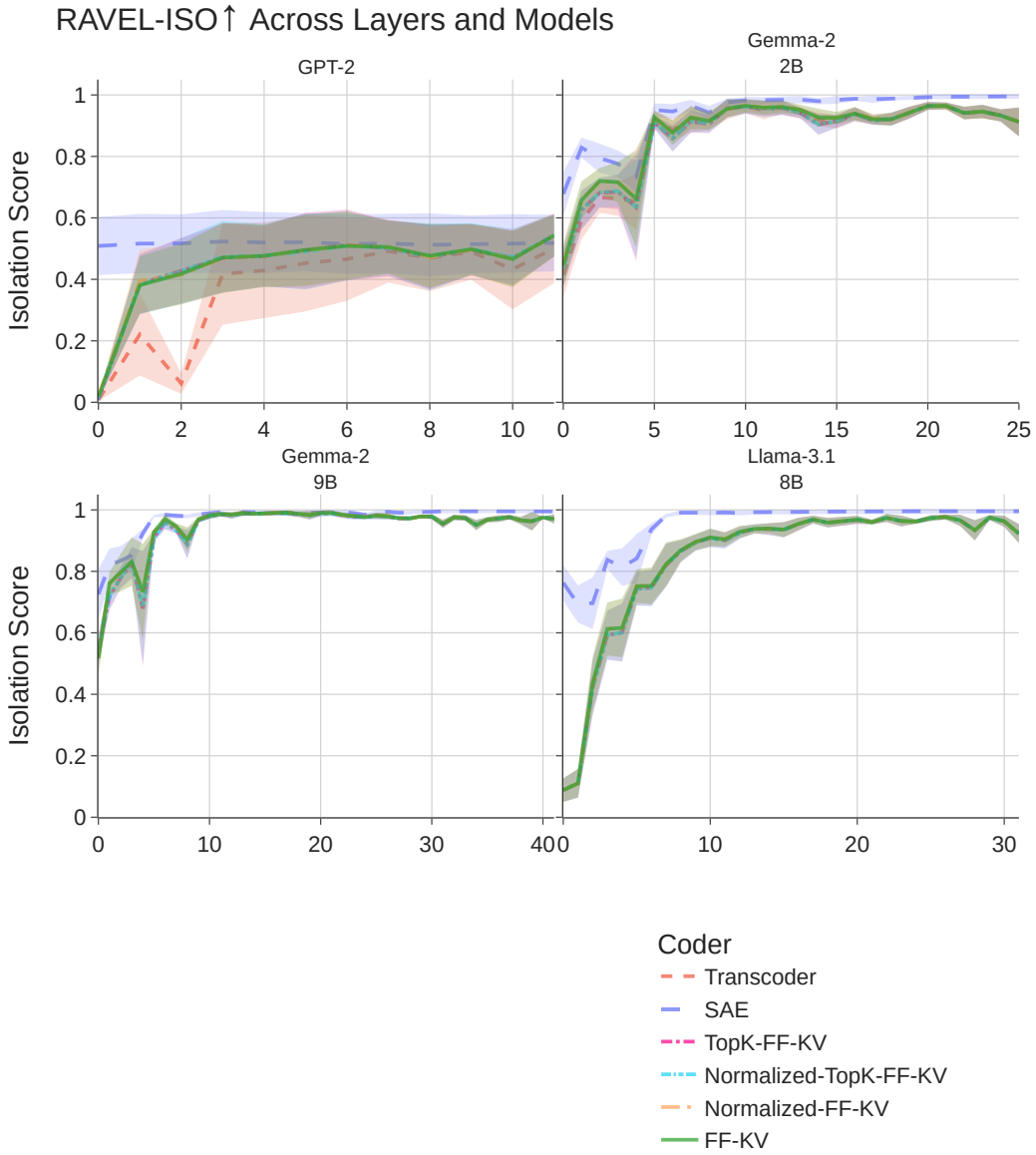


Figure 8: Detailed RAVEL scores on all tested models, across all layers.

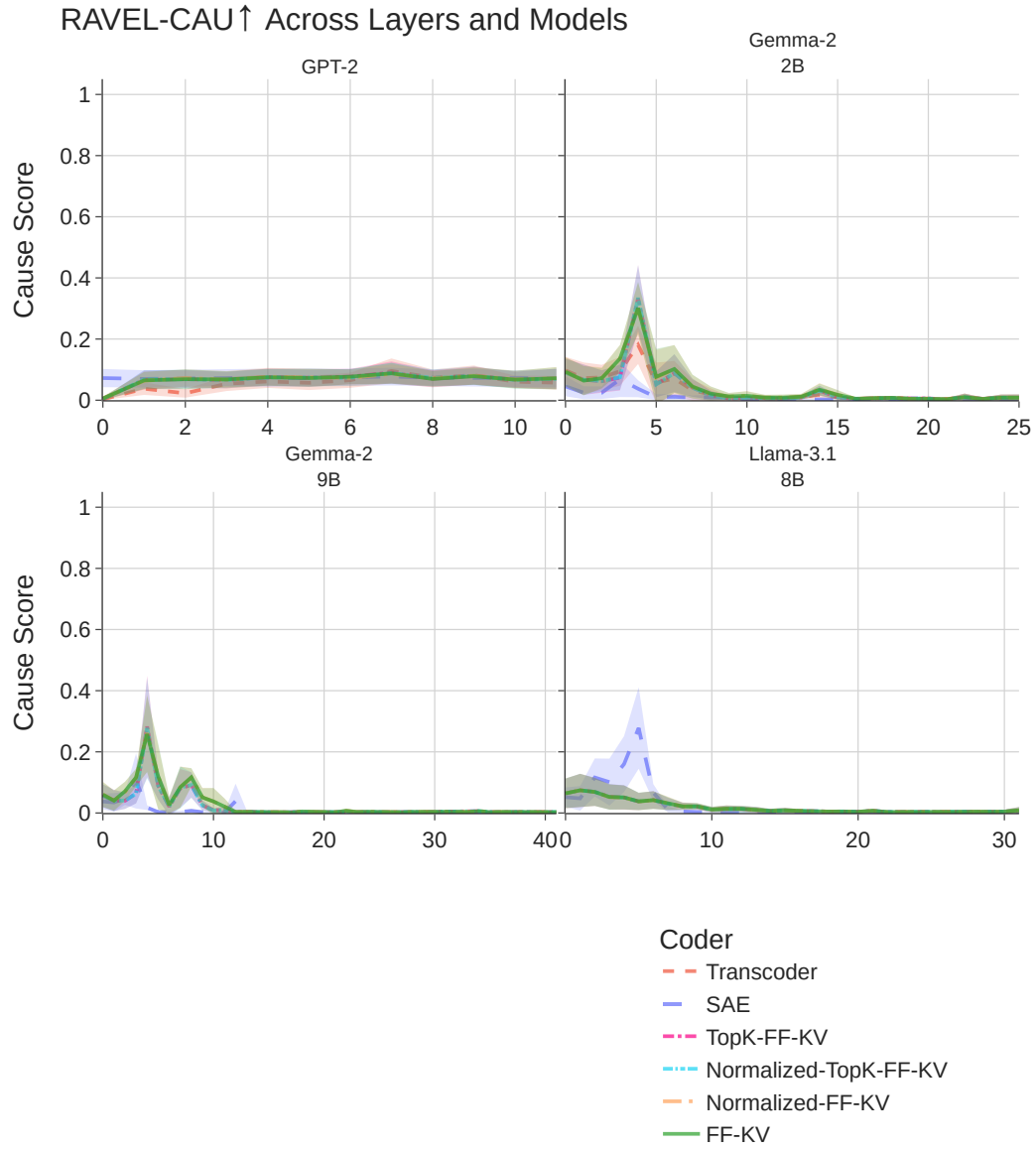


Figure 9: Detailed RAVEL scores on all tested models, across all layers.

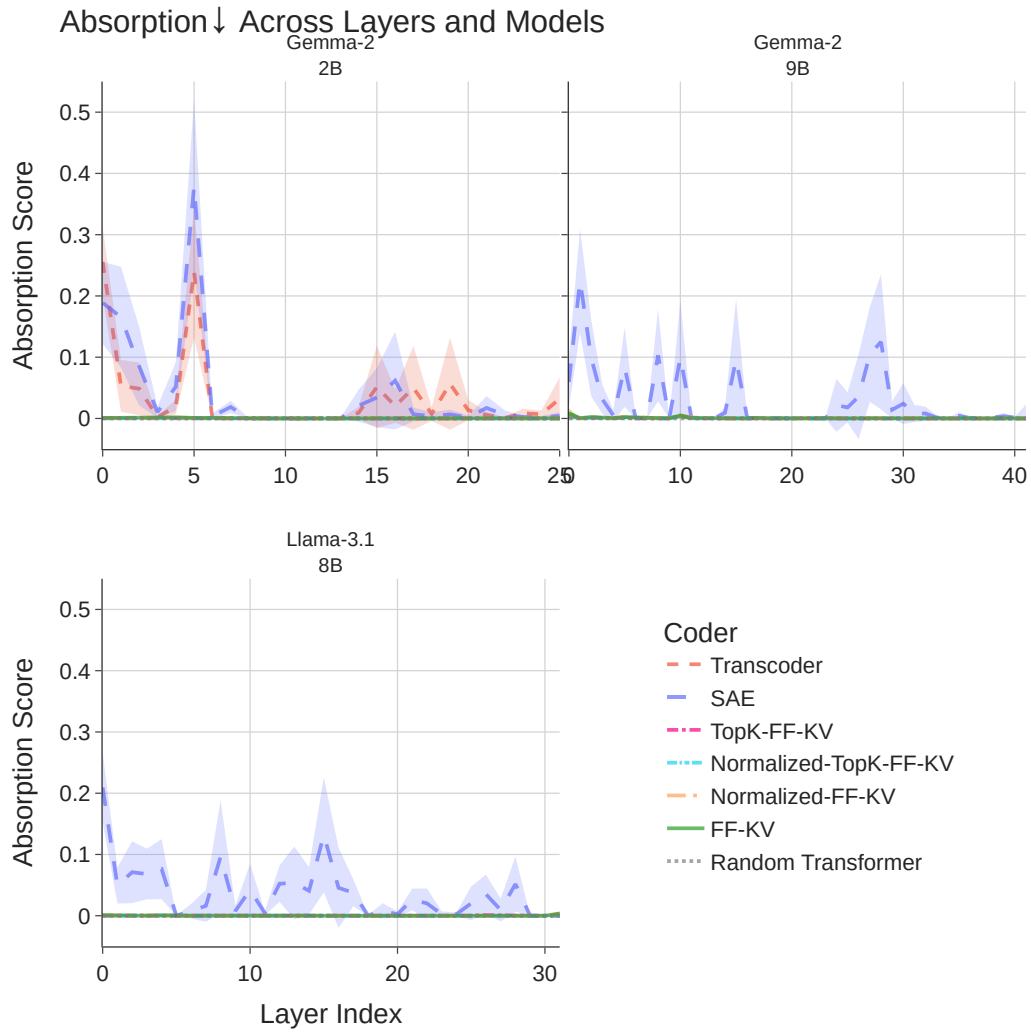


Figure 10: Detailed absorption scores on all tested models, across all layers.

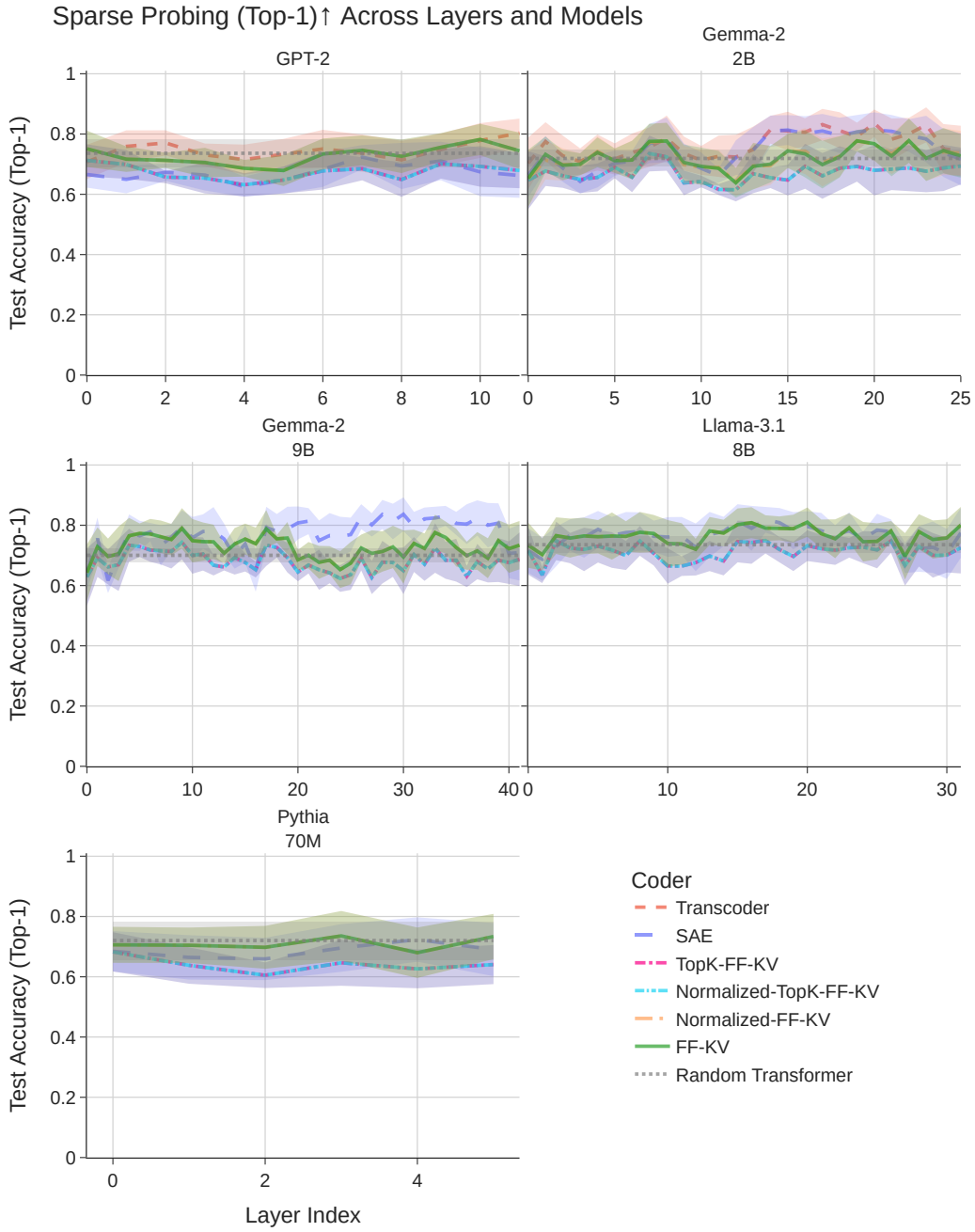


Figure 11: Detailed sparse probing scores on all tested models, across all layers, and various hyperparameter ( $K$ ) choices.

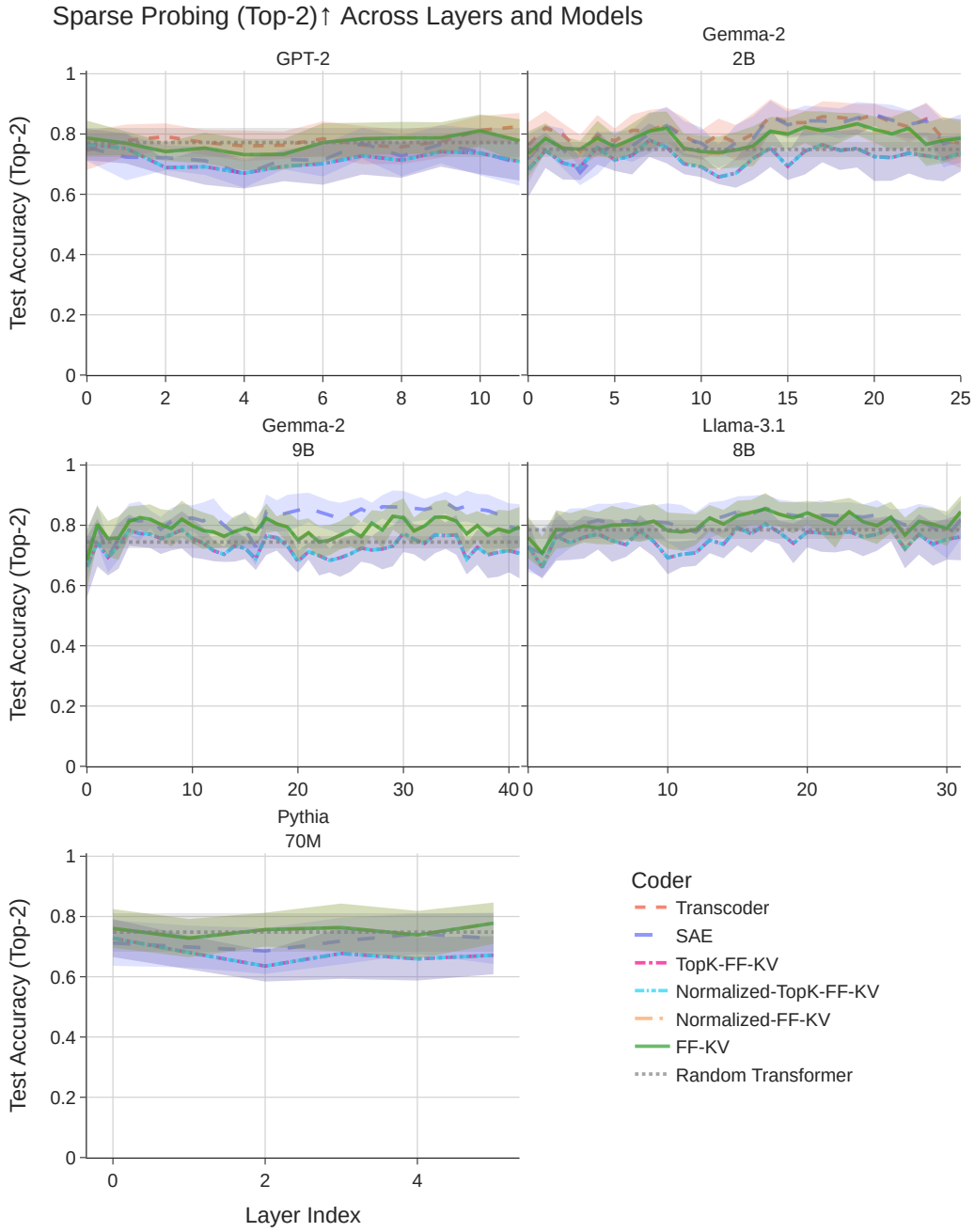


Figure 12: Detailed sparse probing scores on all tested models, across all layers, and various hyperparameter ( $K$ ) choices.

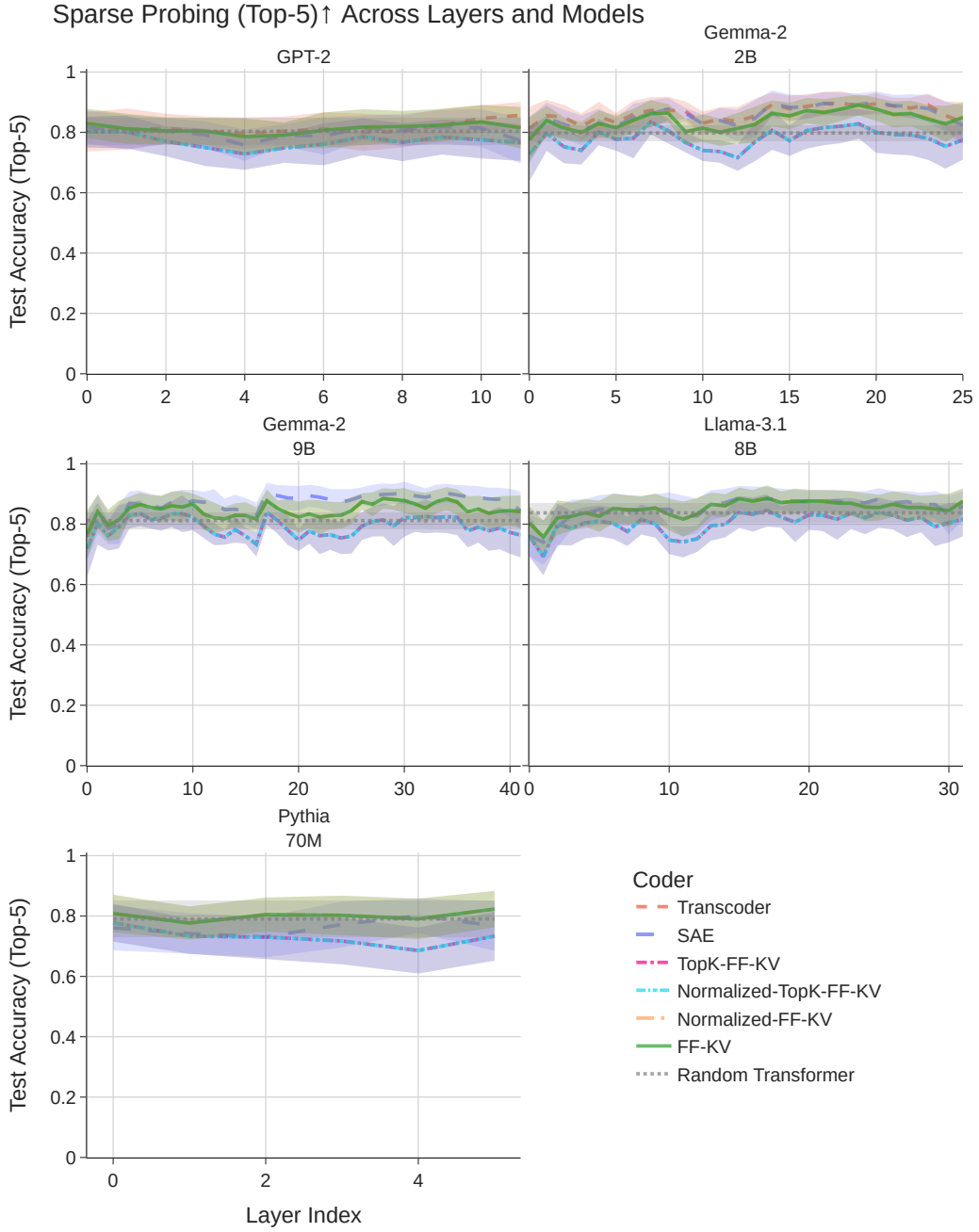


Figure 13: Detailed sparse probing scores on all tested models, across all layers, with **the same hyperparameter choice** as the main result in Table 1.

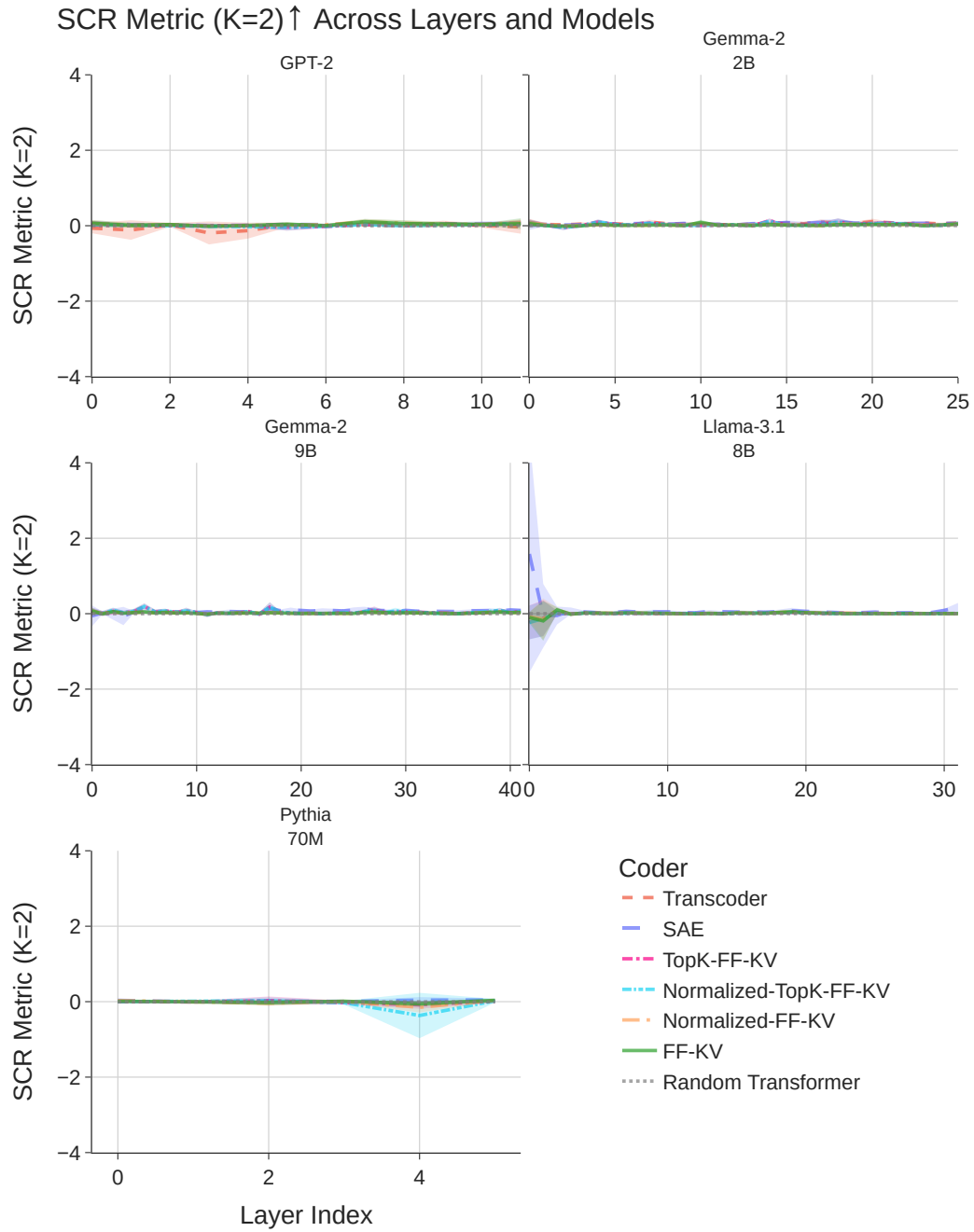


Figure 14: Detailed SCR scores on all tested models, across all layers, and various hyperparameter ( $K$ ) choices.

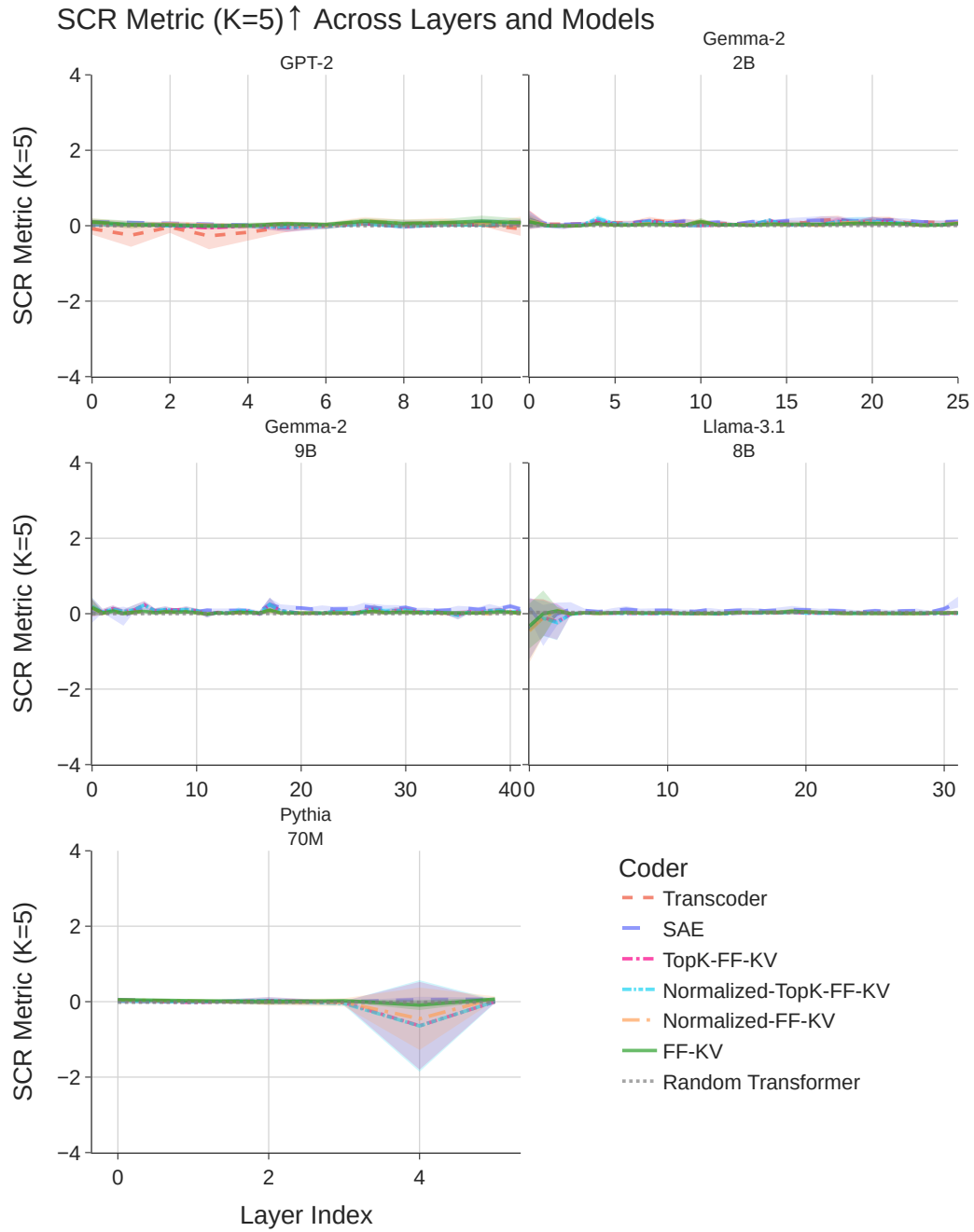


Figure 15: Detailed SCR scores on all tested models, across all layers, and various hyperparameter ( $K$ ) choices.

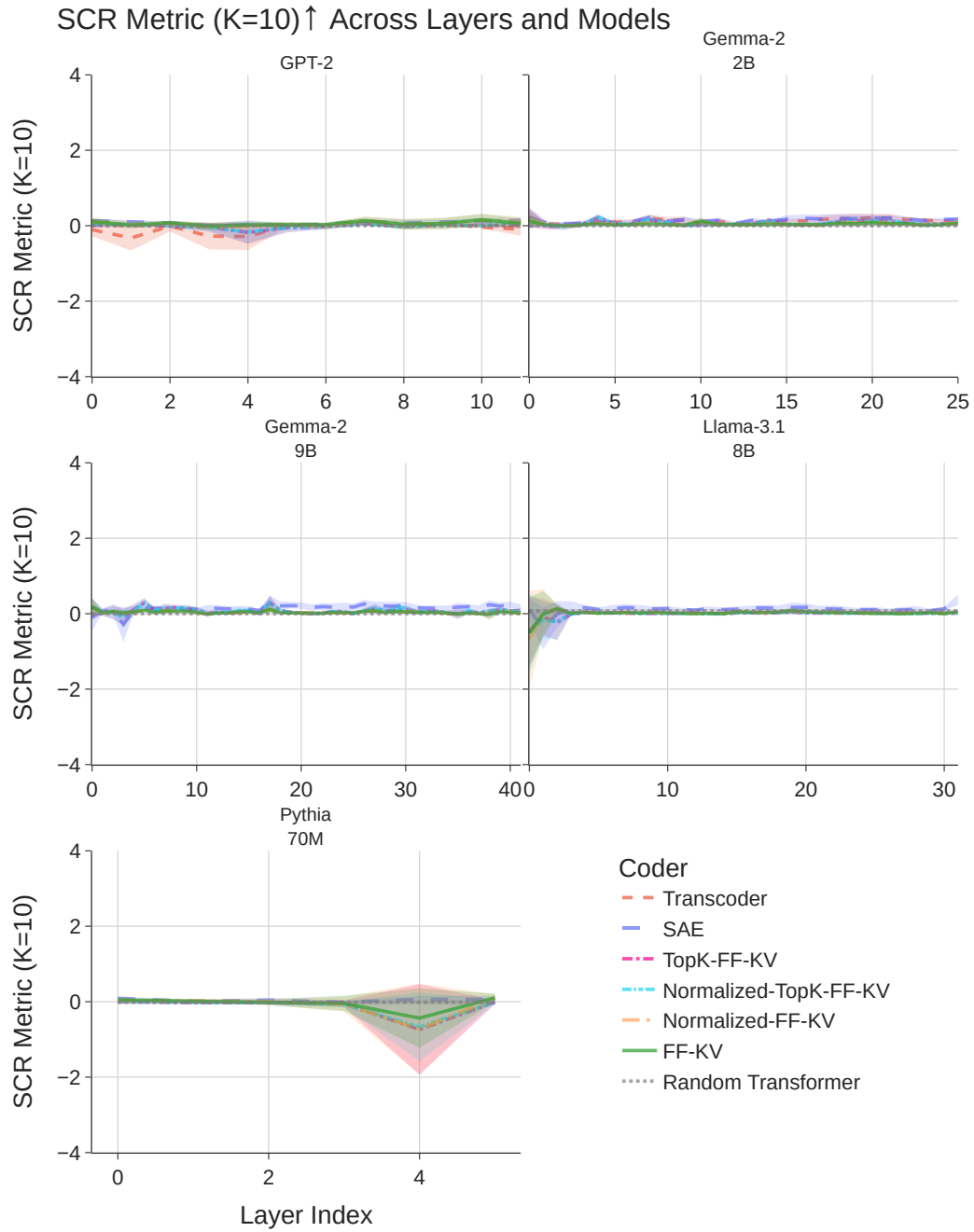


Figure 16: Detailed SCR scores on all tested models, across all layers, and various hyperparameter ( $K$ ) choices.

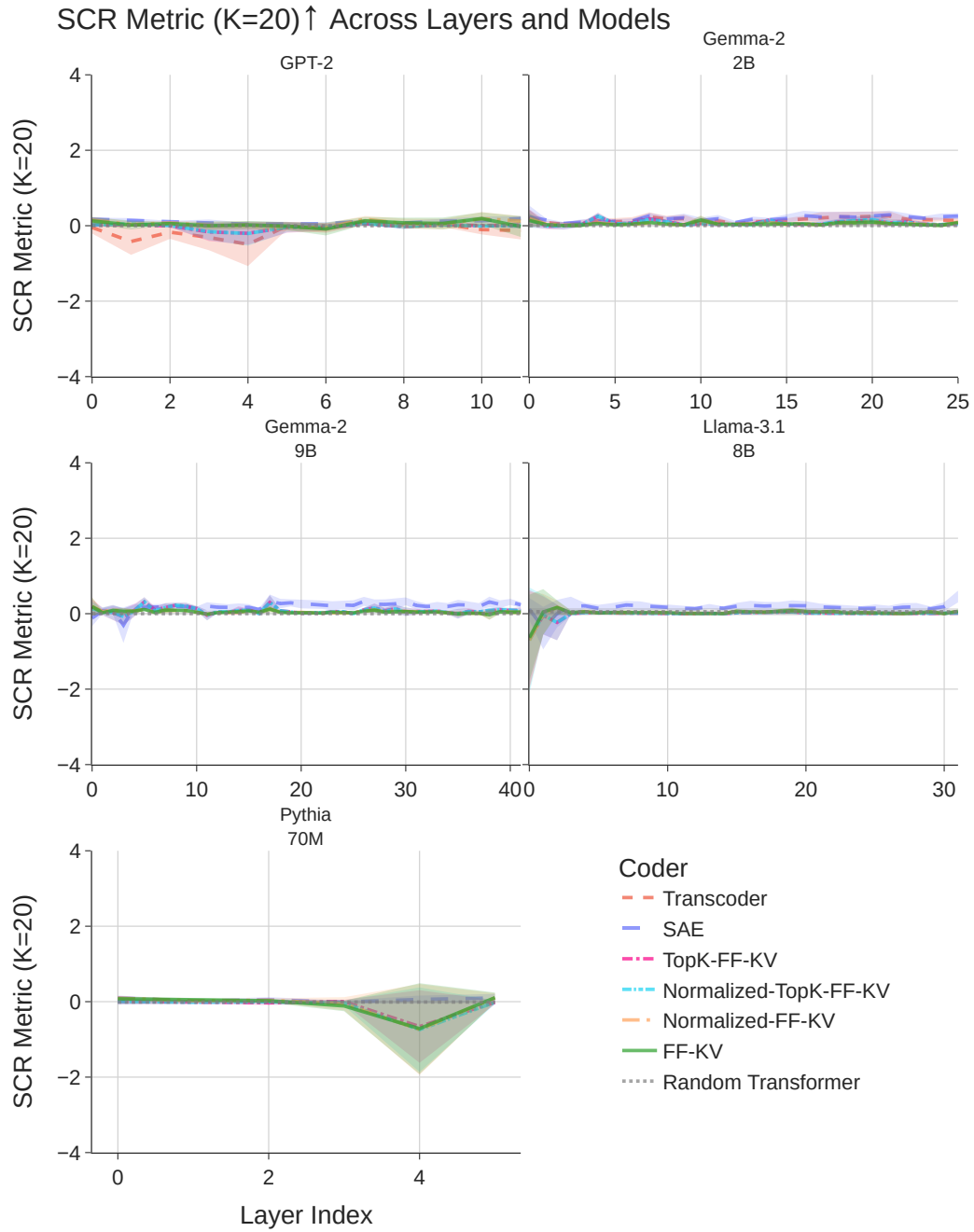


Figure 17: Detailed SCR scores on all tested models, across all layers, with **the same hyperparameter choice** as the main result in Table 1.

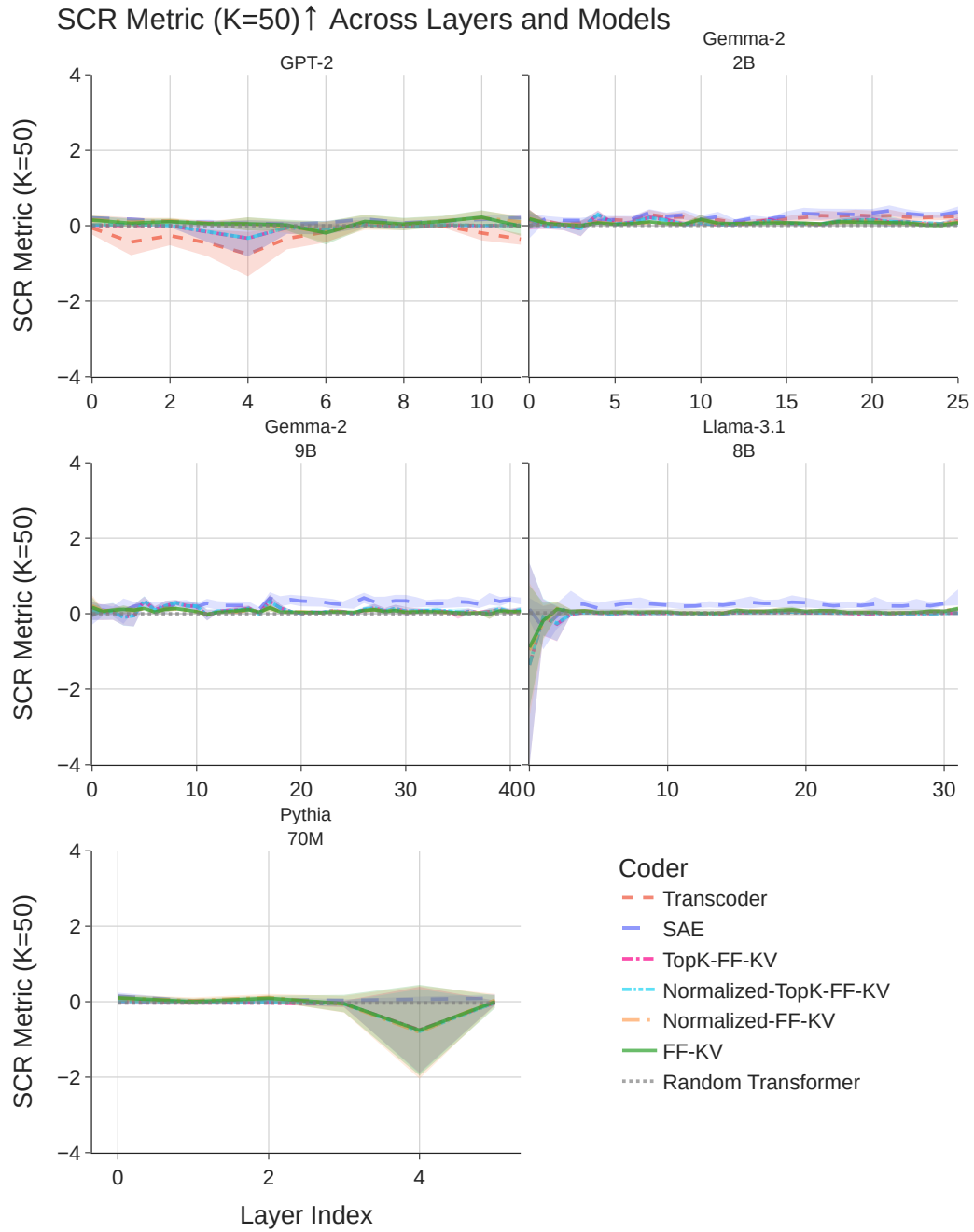


Figure 18: Detailed SCR scores on all tested models, across all layers, and various hyperparameter ( $K$ ) choices.

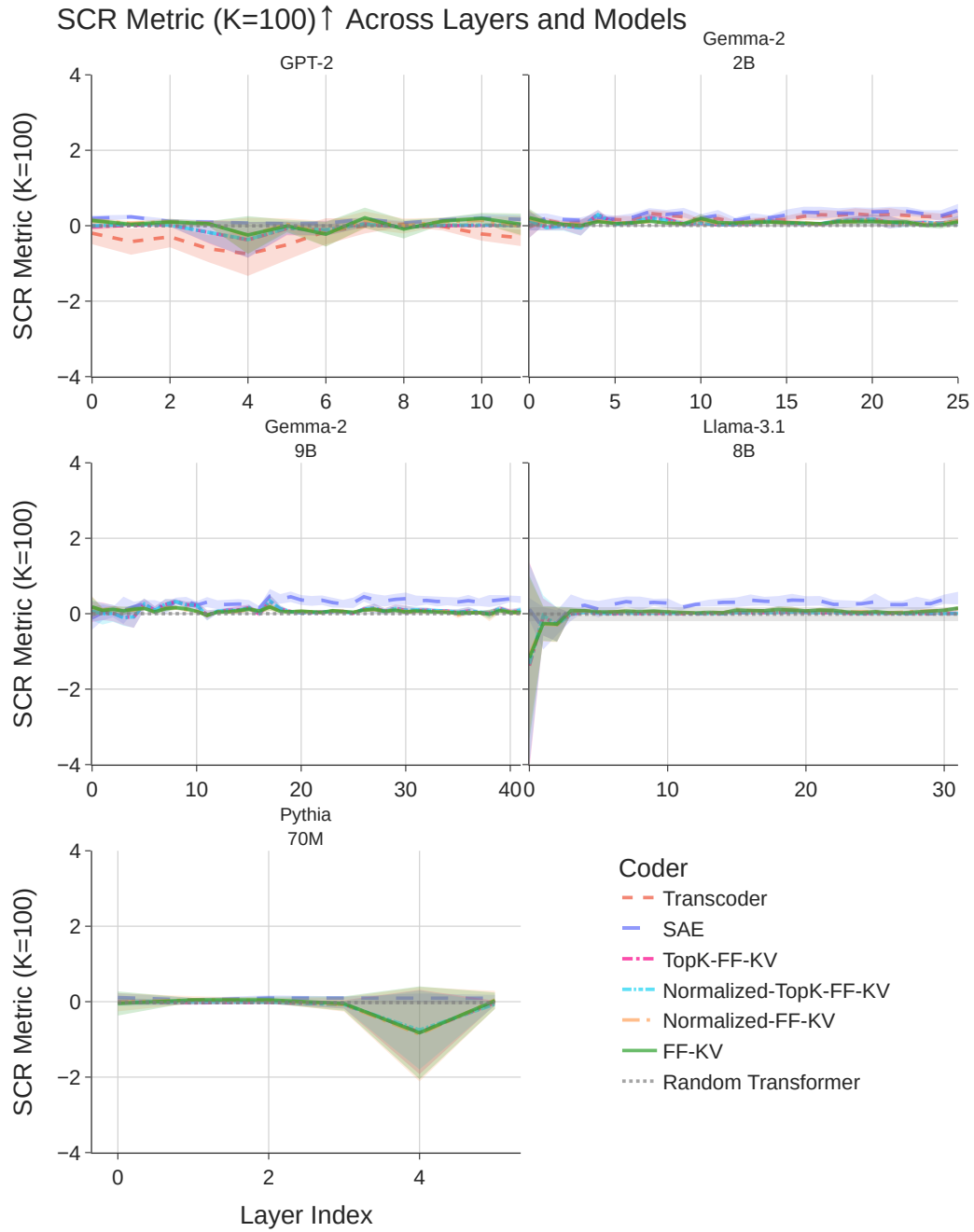


Figure 19: Detailed SCR scores on all tested models, across all layers, and various hyperparameter ( $K$ ) choices.

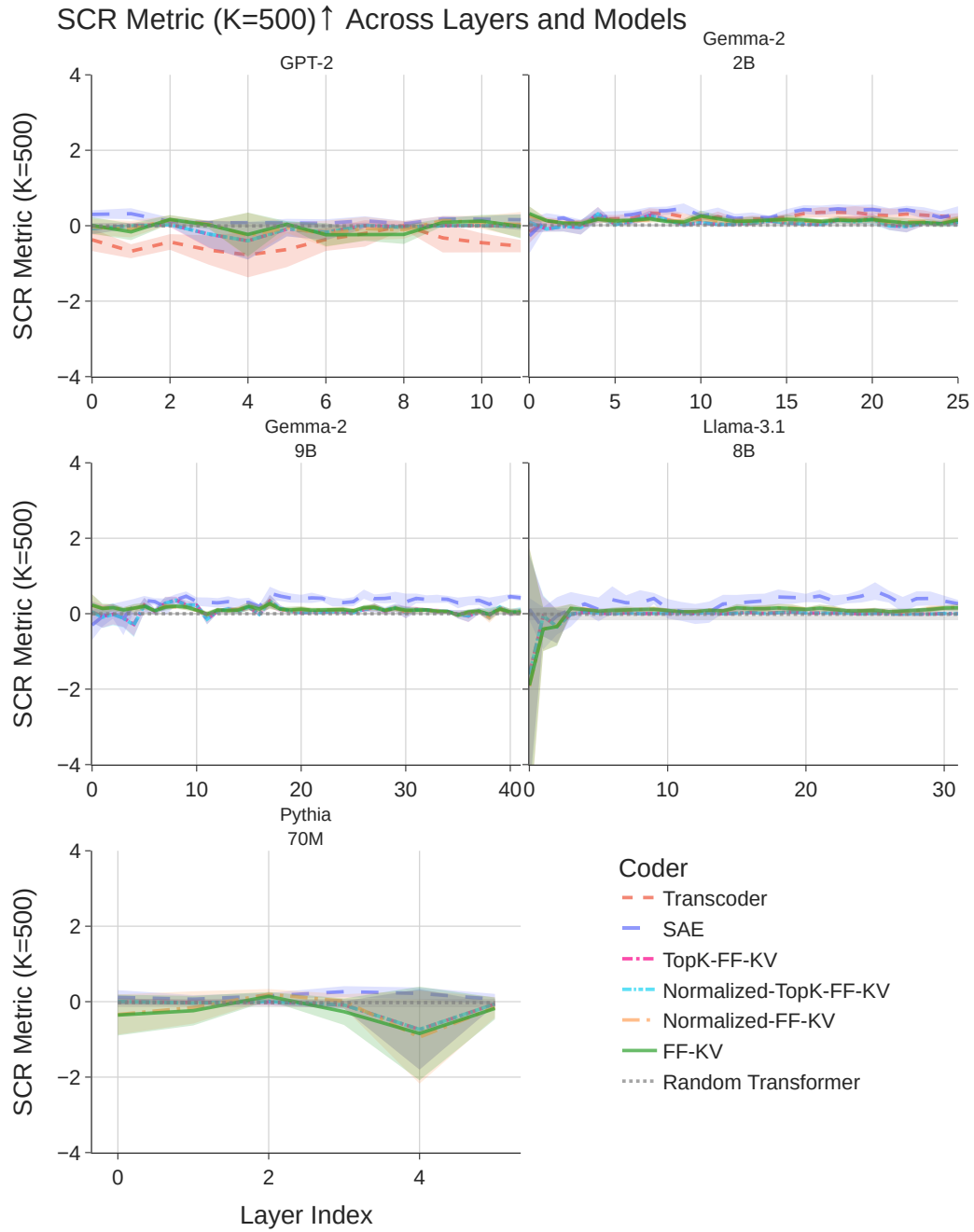


Figure 20: Detailed SCR scores on all tested models, across all layers, and various hyperparameter ( $K$ ) choices.

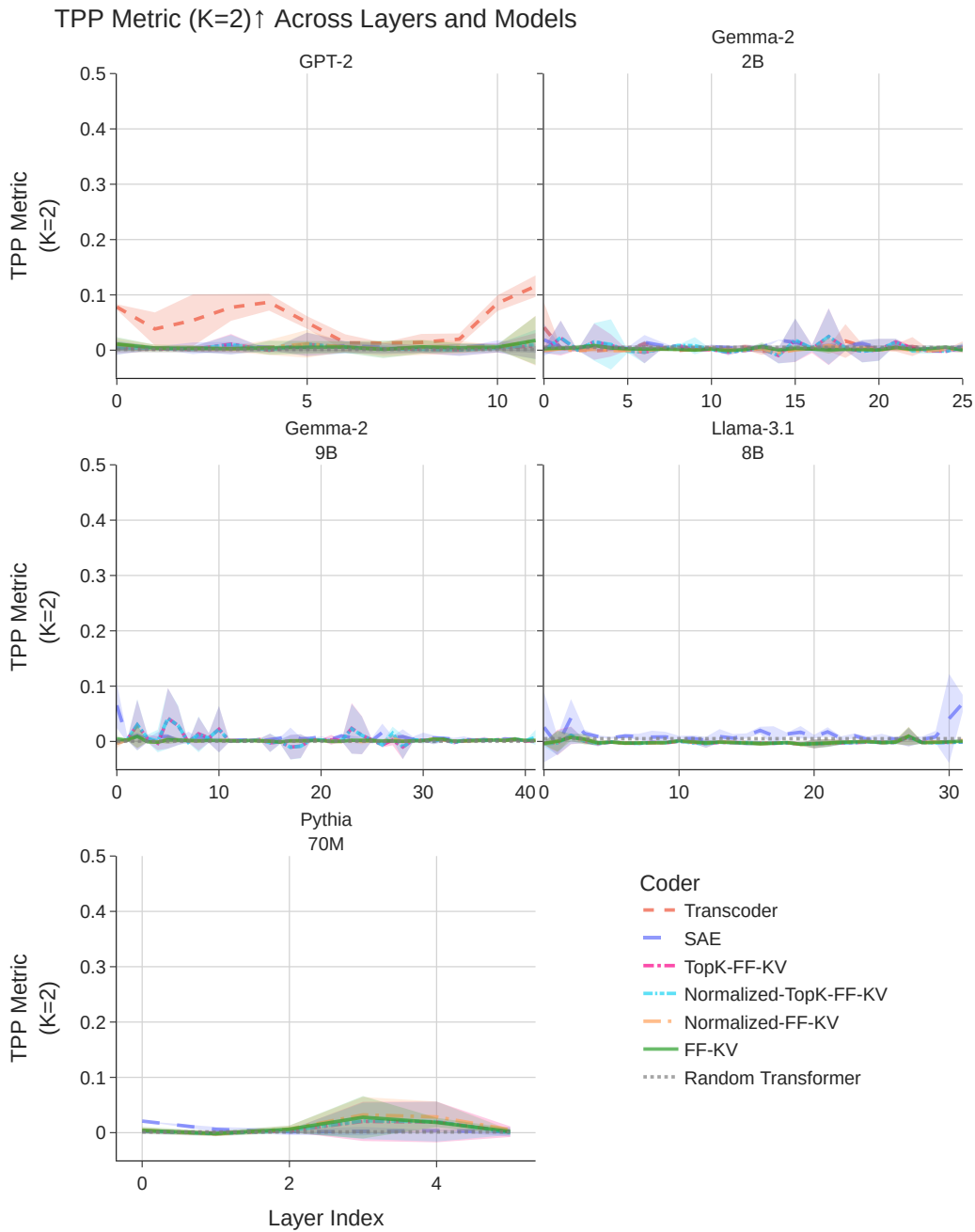


Figure 21: Detailed TPP scores on all tested models, across all layers, and various hyperparameter ( $K$ ) choices.

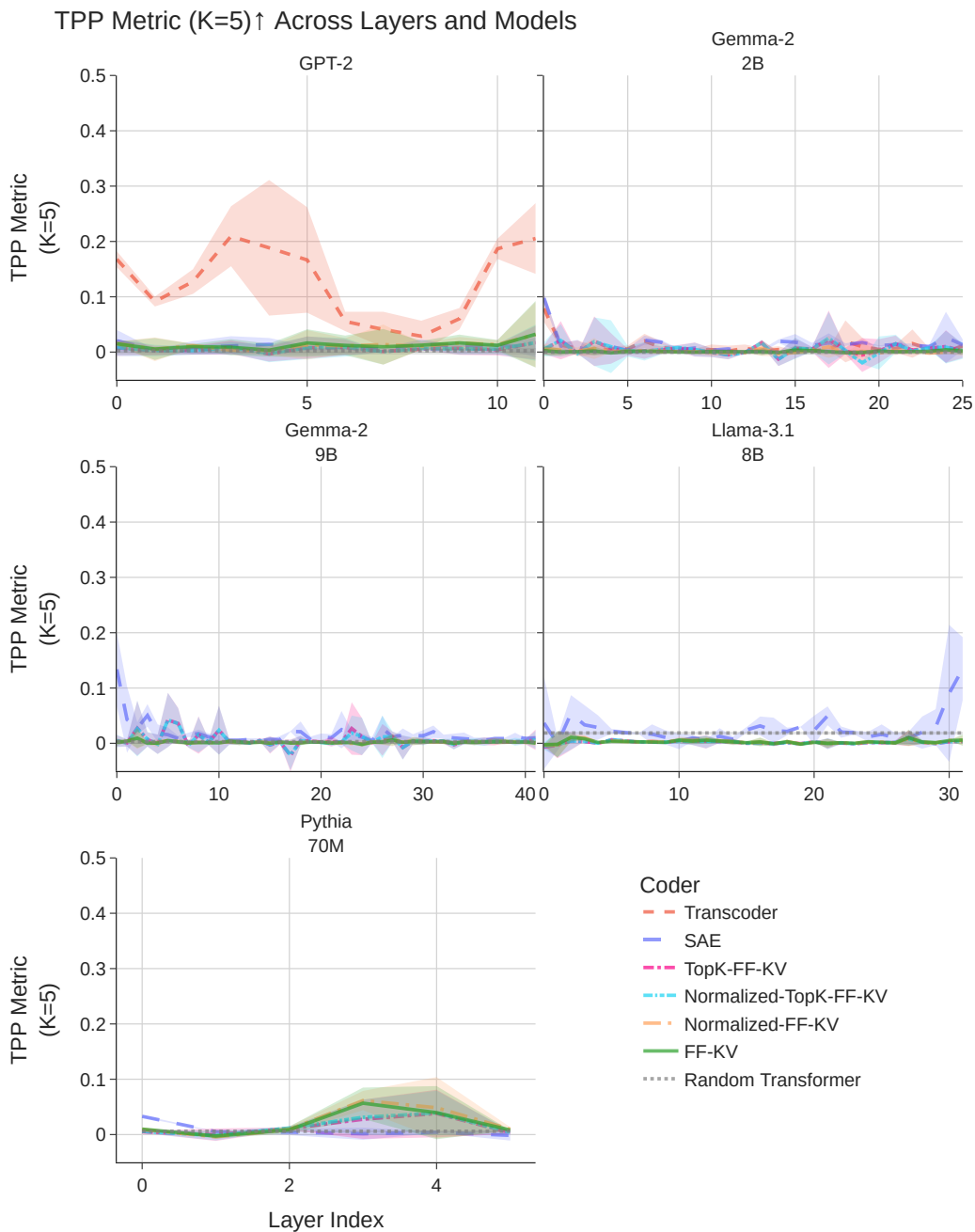


Figure 22: Detailed TPP scores on all tested models, across all layers, and various hyperparameter ( $K$ ) choices.

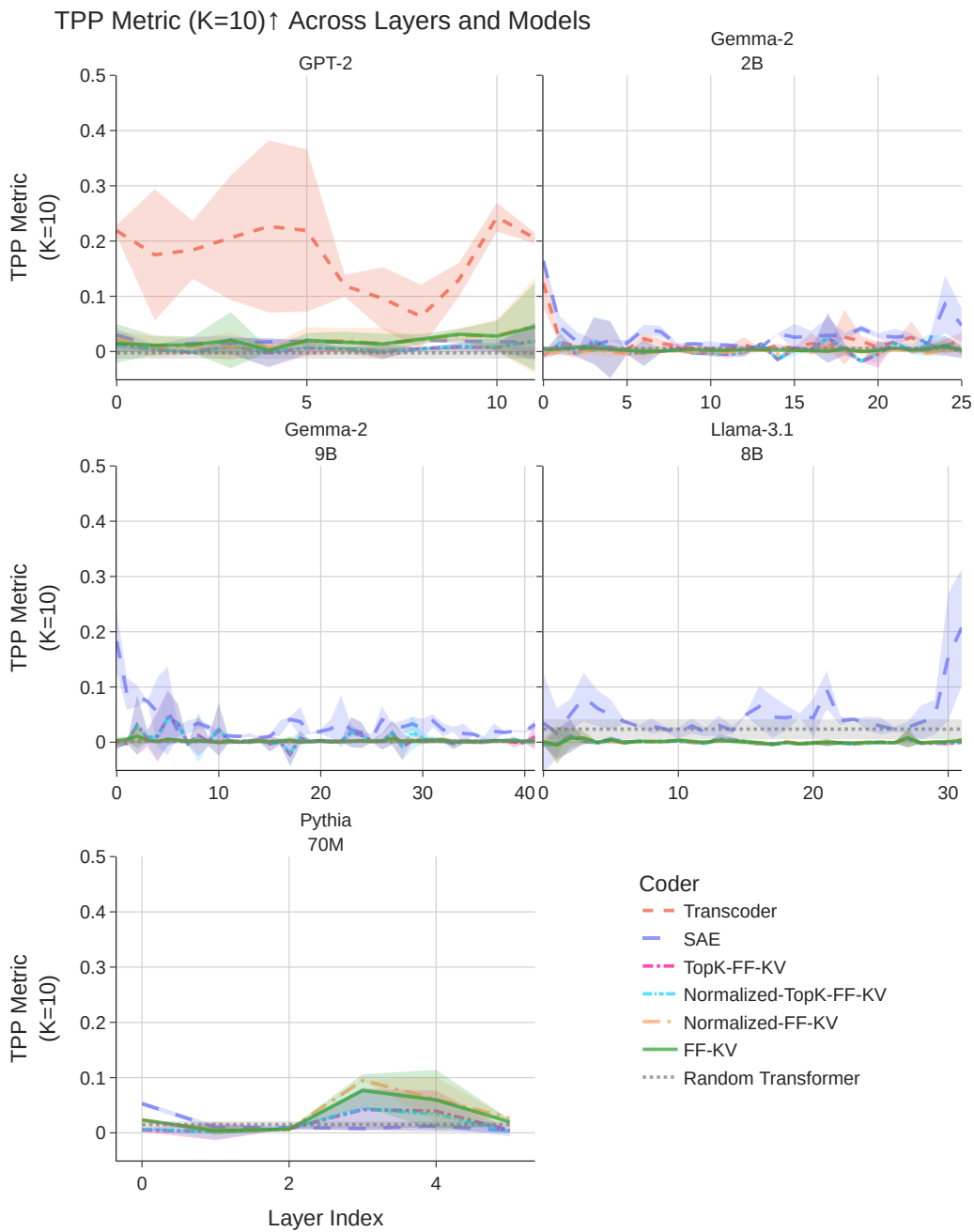


Figure 23: Detailed TPP scores on all tested models, across all layers, and various hyperparameter ( $K$ ) choices.

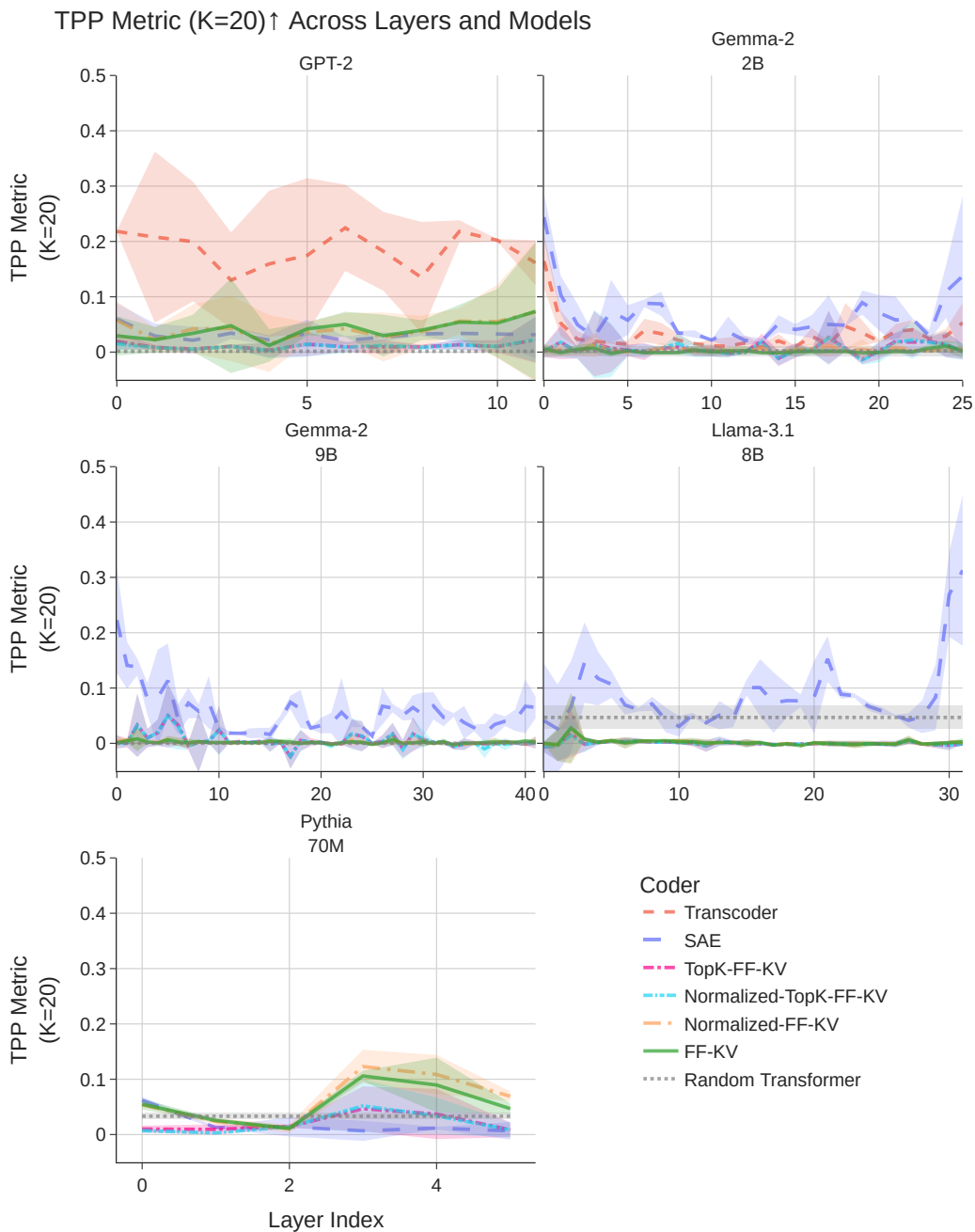


Figure 24: Detailed TPP scores on all tested models, across all layers, with **the same hyperparameter choice** as the main result in Table 1.

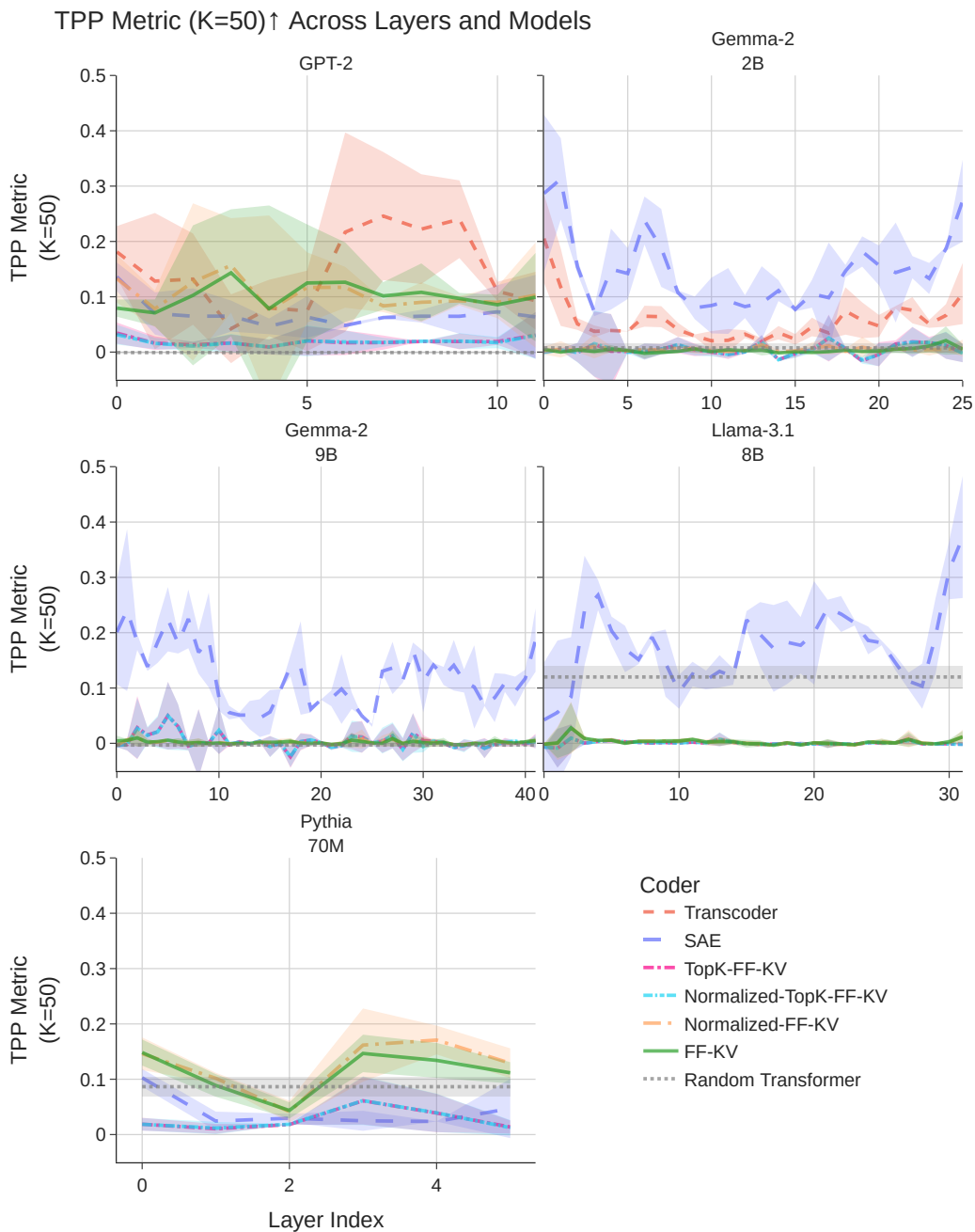


Figure 25: Detailed TPP scores on all tested models, across all layers, and various hyperparameter ( $K$ ) choices.

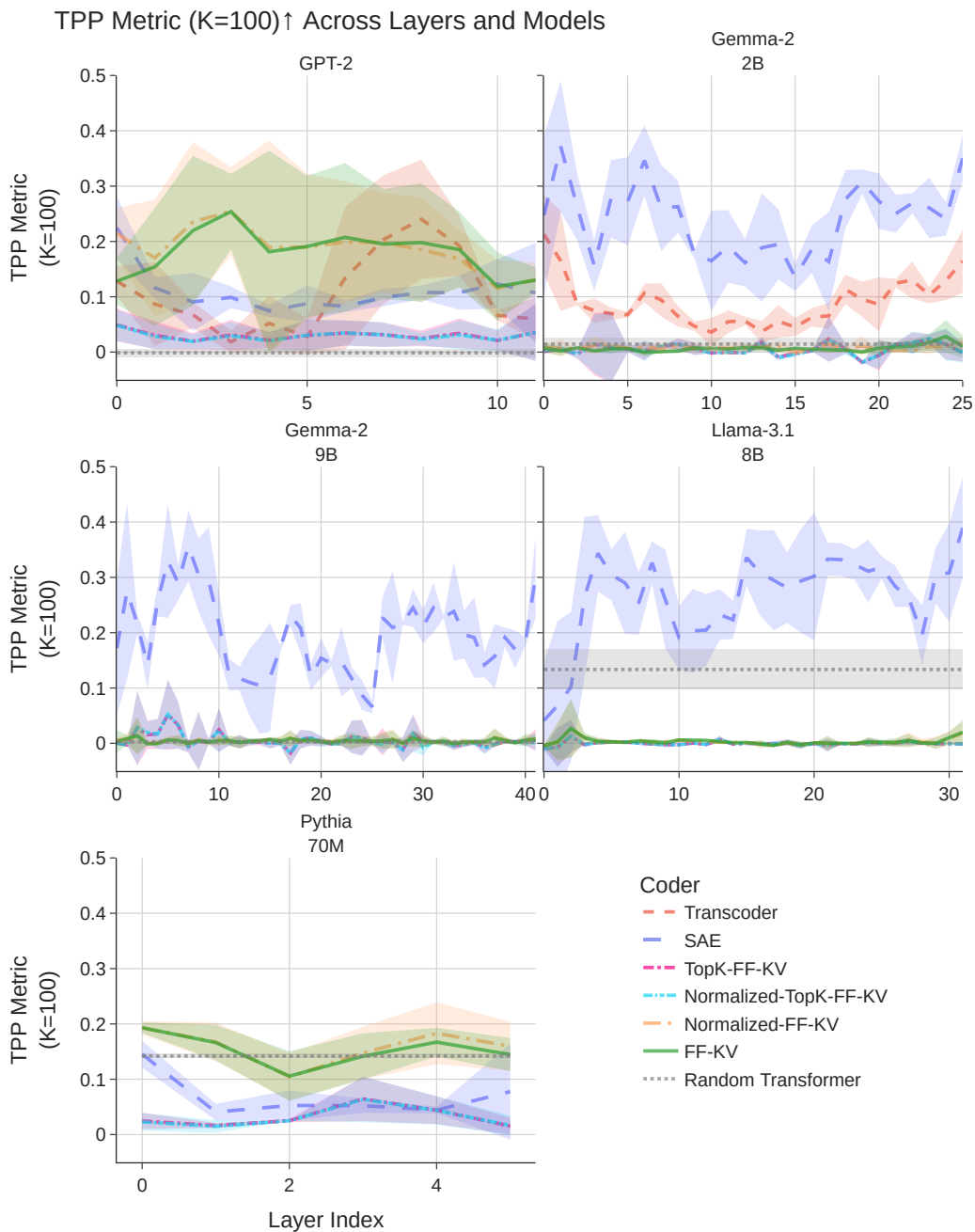


Figure 26: Detailed TPP scores on all tested models, across all layers, and various hyperparameter ( $K$ ) choices.

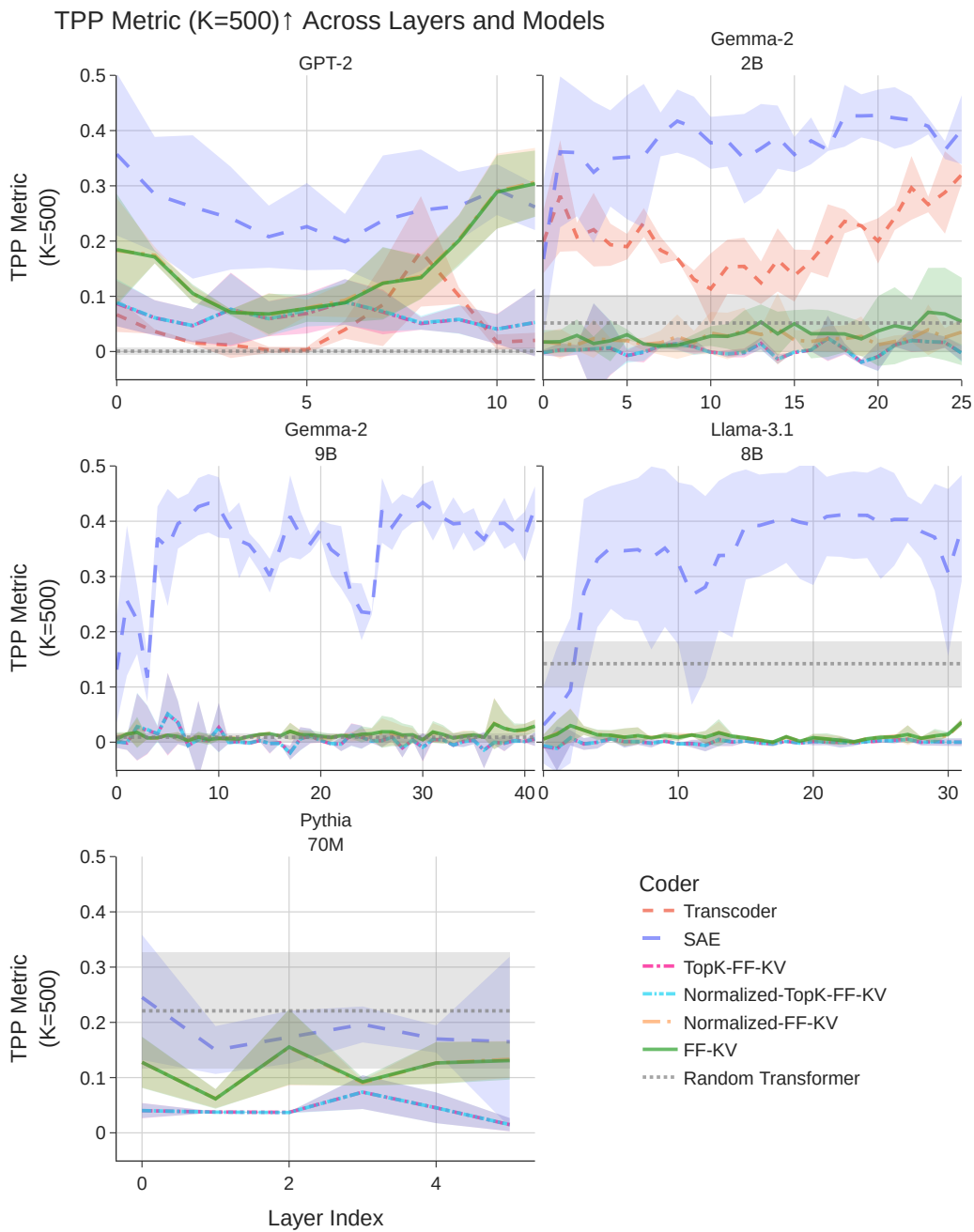


Figure 27: Detailed TPP scores on all tested models, across all layers, and various hyperparameter ( $K$ ) choices.

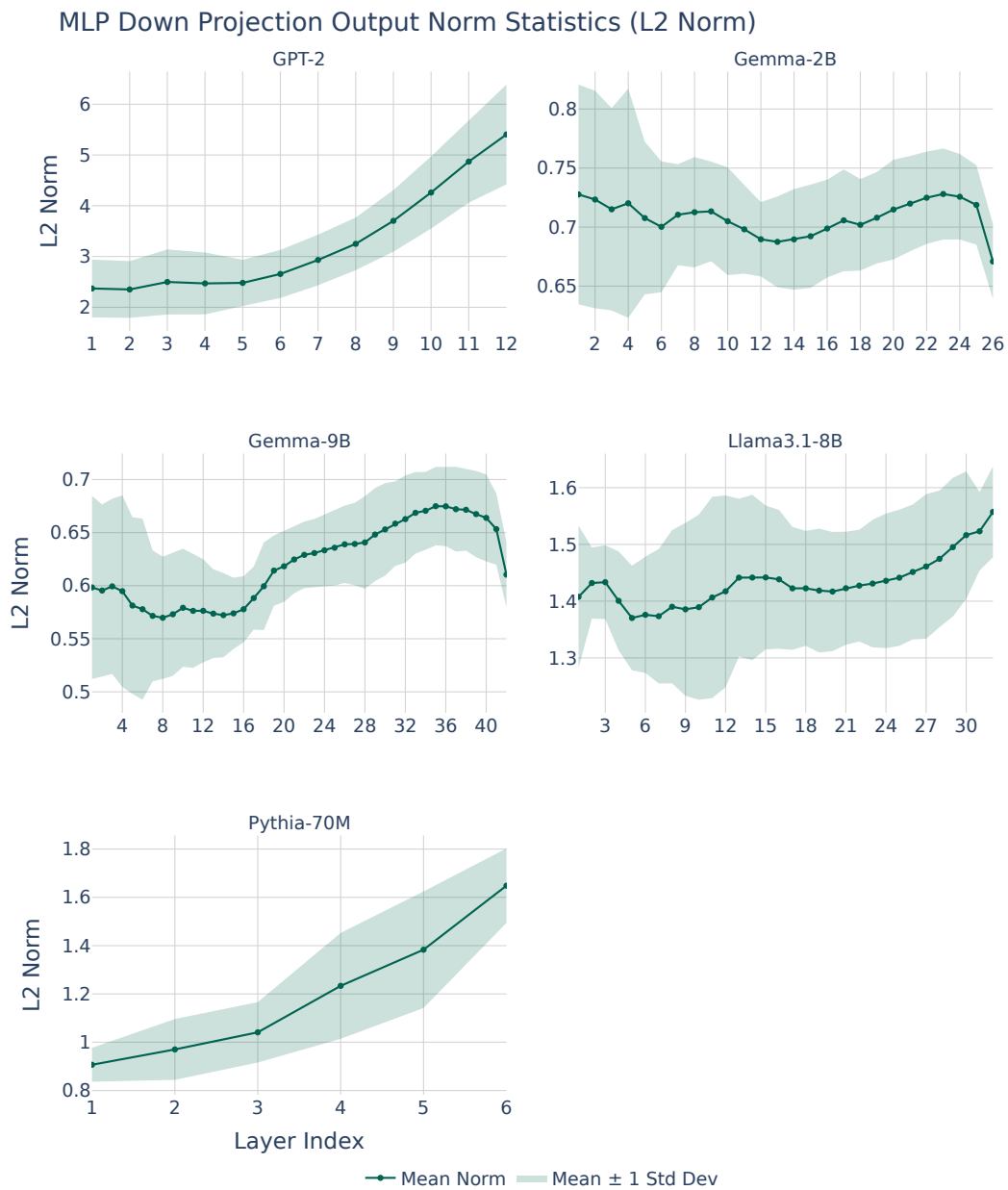


Figure 28: Distribution of the L2 norms of all tested models' FF-KV decoder weights (i.e.,  $\mathbf{W}_2$  in its FF sublayer). Although the norms are not exactly one, they are concentrated in a narrow range.

Text ID: 6269 (Max Activation: 0.691)

that the unemployment rate is actually 14.4 percent. This number includes about 800,000 discouraged workers who have given up seeking employment and roughly eight million workers who are in part-time jobs but would prefer to work a full-time job. "The unemployment rate now stands at 7.9 percent. To put this number in perspective, while that's a big improvement from the 10 percent reached in late 2009, it is now higher than unemployment ever got in the 24 years before the Great Recession," said Yellen in her prepared remarks.

Text ID: 962 (Max Activation: 0.629)

despite all the electoral spending, Ruth Davidson's Conservatives (TM) won just 13 seats out of 59. They fought the election on the single issue of opposition to another independence referendum, and they still lost. Improving on the number of seats you achieved still doesn't make you a winner, any more than improving your results in an arithmetic exam from an F to a D means that you're now top of the class. Scotland looked at Ruth Davidson's party and still gave them a failing grade – all the Tory triumphalism in the world won't change that simple arithmetic reality.

Text ID: 2495 (Max Activation: 0.520)

're moving a piece of functionality out of a method that's doing too many things, it's very likely that the original method now has extra references that just aren't needed anymore. In the midst of the refactoring, you may be so focused on the extraction, that you forget to clean these bits up. And, by cleaning it up, you may uncover a trail of other code that can go into the trash bin as well. Without this cleanup, you've just added the debt of useless code to your system. That might make the newly refactored code base just as hard to read.

Text ID: 14099 (Max Activation: 0.500)

He struggled to continue the paper, and though he asked for help, [11] he received none. The home of Travis and Rosanna, relocated to Perdue Hill, Alabama and restored in 1985. On February 27, 1829, Travis passed his law examination and received permission to legally practice, so he borrowed \$55.37 to open a law office, [12] as well as \$90 earlier in the year to help pay for the Herald, [13] Now in debt and with no practical income, he took in three boarding students, and to help

Figure 29: Top-4 activating examples for a particular feature in FF-KV annotated as “superficial”. This feature specifically activates most on the word “now”, in various contexts.

Text ID: 11936 (Max Activation: 2.609)

Claudio Ranieri as coach of the first team. " Following this move, **the** financial contract with Ranieri, whose deal was coming to an end on 30 June 2011, has ended by mutual consent. Roma wishes to thank Claudio Ranieri for the professionalism shown and the work done [ during his time at the club ]." Ranieri enjoyed a successful first season with Roma after replacing Luciano Spalitti in September 2009. **The** club had endured an horrendous start to the campaign and Ranieri, who had been fired by Juventus months earlier, rescued **the** team and nearly led them to the scu

Text ID: 15318 (Max Activation: 2.484)

£ 59.7 m Angel Di Maria -- Real Madrid to Man Utd, Aug. 2014 ( £ 56 m Kaka -- AC Milan to Real Madrid, June 2009 Sources told ESPN FC that Chelsea have been quoted a price of 40 million pounds by PSG for Cavani, and that **the** player is eager to move to Stamford Bridge -- despite a public declaration that he would prefer to stay in France. There has already been preliminary contact between **the** London club and the player's camp, although Chelsea are still assessing **the** best course of action. With Mourinho having regularly complained

Text ID: 7334 (Max Activation: 2.484)

spokesman Adam Rosen said he is ' shocked ' that an agency of first responders would enforce such an order **the** week of Sept. 11. " **The** four suspended firefighters said they were told that **the** order was issued because of racial discord [ in ] the department. **The** four, who include two white firefighters, a black firefighter, and a fourth firefighter who is a Cuban é mig ré, said no such problems exist," wrote CBS, which also reported that **the** four firefighters trace the issue " to a decision by several firefighters to replace a tattered American flag last month in one of Maywood's fire houses. **The** new flag mysteriously

Text ID: 12010 (Max Activation: 2.453)

Trading standards are investigating after a couple who stayed at a hotel claimed to have been " fined " £ 100 by a hotel which they described as a " rotten stinking hotel " on TripAdvisor. Tony and Jan Jenkinson, from Whitehaven in Cumbria, posted a review on the website after staying at the Broadway Hotel in Blackpool. However, **the** couple later found that £ 100 charged to their credit card, which **the** BBC reported was the result of a hotel policy in the case of " bad " reviews. **The** manager of **the** hotel was not available for comment last night. **The** Jenkinsons, who

Figure 30: Top-activating examples for a feature in *k*-Sparse FF-KV annotated as "superficial". This feature specifically activates most on the word "the", in various contexts.

**Text ID: 11353 (Max Activation: 18.412)**

```
k in xrange ( 0 , high + 1 ): p = Eval Poisson P mf ( k , lam ) pm f . Set ( k , p ) pm f . Normalize () return
pm f The range of values in the computed P mf is from 0 to high . So if the value of lam were exactly 3 . 4
, we would compute : lam = 3 . 4 goal _ dist = think bayes . Make Poisson P mf ( lam , 1 0 ) I chose the upper
bound , 1 0 , because the probability of scoring more than 1 0 goals in a game is quite low . That ' s simple
```

**Text ID: 8952 (Max Activation: 17.365)**

```
q - k + 1 ) / k if k <= p : c list . append ( c ) d *= 1 . 0 * ( q - k + 1 ) / ( p + q - k + 1 ) / k if k <= q : d list
. append ( d ) return np . array ( c list [ :- 1 ] ) , np . array ( d list [ :- 1 ] ) def arg box ( y , ymin , ymax , imin , imax
): "" find limits ( we hope ) where y [ i ] is between ymin and ymax "" ii = np . arg where ( np . logical _ and ( y
> ymin , y < ymax )) ii = ii
```

**Text ID: 4503 (Max Activation: 17.178)**

```
asm __ ( " f sel % 0 , % 1 , % 2 , % 3 " : "= f " ( result ) : " f " ( test ) , " f " ( b ) , " f " ( a ) ); return
```

**result** ; } Such optimizations are implementation details , but are described here because they provide a practical performance benefit to the performance - conscious user . It would be nice if std STL implementations provided such

things , though Met rower ks has been known to do so in some cases . Instead of just < algorithm > , EAST L has < algorithm . h > , < sort . h > , < algo set . h > ,

**Text ID: 10231 (Max Activation: 16.843)**

```
1 0 0 0 0 0 0 0 % 1 0 + i 1 / 1 0 0 0 % 1 0 + i 1 / 1 0 % 1 0 )) % 1 0 ) % 1 0 + 1 0 * i
0 ; printf ( "% d " , i 2 ); return ( 0 ); } user @ kali : ~$ gcc - o d link - wps - gen quanta - wps - gen . c
user @ kali : ~$ ./ d link - wps - gen 9 7 3 2 9 3 2 9 user @ kali : ~$ You can fetch this program at https ://
```

**Text ID: 9000 (Max Activation: 14.418)**

```
. complex 1 2 8 ) S [ , k ] = ( np . roots ( Q plus ) - np . roots ( Q minus ) ) / roots / delta if not extras : return
S # extras : find a direction of maximum sensitivity u , s , v = np . linalg . svd ( S , compute _ uv = True ) #
largest singular direction in reverse order # to match polynomial coefficients n - 1 : 0 return S , s [ 0 ] , v [ 0 , :- 1
] S , kappa , v = find _ root _ sen siti vities ( Q , extras = True ) S , kappa , v ( array ( [ - 0
```

Figure 31: Top-activating examples for a feature in SAE annotated as “superficial”. This feature activates on the word “return”, especially in programming-related contexts.

**Text ID: 4591 (Max Activation: 34.000)**

might be worth using as a reference . A full discussion of compiler in lining characteristics is outside the scope of this document , but some Internet discussions regarding GCC in lining problems can be found at : http :// groups . google . com / group / comp . lang . c ++ / browse \_ frm / thread / b 7 4 eed 1 6 bd 4 8 d 4 2 e http :// groups . google . com / group / fa . linux . kernel / browse \_ frm / thread / 1 8 6 1 b 2 6 3 4 cd fa 6 8 a / http :// www . pixel glow . com / lists / archive

**Text ID: 3930 (Max Activation: 33.750)**

buy all of the parts needed , including the plastic case , knob , and AC adapter . You can edit your cart after loading the project if you want to change anything . To access the shared project , go to http :// www . m ouser . com / Project Manager / Project Detail . aspx ? Access ID = b 6 8 a 3 0 2 3 1 c or http :// www . m ouser . com / Tools / Tools . aspx and enter this access code : b 6 8 a 3 0 2 3 1 c Upgrades I am often asked what can be done to upgrade the designs that I publish . In this case , there

**Text ID: 6968 (Max Activation: 32.250)**

an environment variable JE BIO \_ API KEY , or pass it as a parameter if you are importing the script as a library ). Queries return JSON output , except for download requests , that return binary attachments . The return " code " variable is set to 0 on success , != 0 on error . Here are a few examples : Query a file hash : \$ jeb io . py check 4 2 aaa 9 3 a 8 9 4 a 6 9 bf cbc 2 1 8 2 3 b 0 9 e 4 ea 9 f 7 2 3 c 4 2 8 4 2 aaa 9 3 a 8 9 4 a 6

**Text ID: 6971 (Max Activation: 31.500)**

asta . apk " } } Note : the user details section is present only if you up lola ded the file yourself . Upload a file : \$ jeb io . py upload 1 . apk 1 . apk : { " code " : 0 , " uplo ade ven tid " : 1 5 5 } Download a file : ( subject to permission ) \$ jeb io . py download a 2 ba 1 b acc 9 9 6 b 9 0 b 3 7 a 2 c 9 3 0 8 9 6 9 2 bf 5 f 3 0 f 1 d 6 8 a 2 ba 1 b acc 9 9 6 b

Figure 32: Top-activating examples for a feature in **Transcoder** annotated as “superficial”. This feature activates on the combination of digits and alphabet, in various contexts.

Text ID: 6561 (Max Activation: 1.891)

of the Canadian mainland is Point Pelee, Ontario. [ 4 7 ] The western most point is Boundary Peak 1 8 7 ( 6 0 ° 1 8 ' 2 2 . 9 2 9 " N , 1 4 1 ° 0 0 ' 7 . 1 2 8 " W ) at the southern end of the Yukon - Alaska border which is roughly following 1 4 1 ° W but leans very slightly east as it goes North. [ 4 8 ] [ 4 7 ] The eastern most point is Cape Spear, Newfoundland ( 4 7 ° 3 1 ' N , 5 2 ° 3 7 ' W ). [ 4

Text ID: 9818 (Max Activation: 1.617)

positions as a result. Joaquin will move northward much of this weekend, roughly paralleling the East coast. There is nearly equal possibility the storm will make land fall along the mid-Atlantic coast, the New England coast or veer out to sea. Due to the potential close proximity of the hurricane to the coast, people from the Carolinas to Massachusetts will need to closely monitor the track and strength of Joaquin for high wind and coastal flooding concerns. Should Joaquin make land fall, areas near and north of the center would face the worst coastal flooding and strong winds. If the storm were to make land fall in North Carolina

Text ID: 12657 (Max Activation: 1.547)

cop asked him why he wasn't driving. He said he didn't have a truck and a horse trailer, just a horse, a pack horse and a dog. His plan was simply to ride the coast to San Diego and turn left. He had what he called a "shoulder pass" which he drew from his pocket and presented to the officer. The officer, being confused, was not even sure such a document existed and examined its molecular structure. Then the Laguna Animal Control officer showed up. That officer informed the cow poke that he did not have his dog on a leash. Something all good little citizens of California

Text ID: 13010 (Max Activation: 1.531)

picked up from the Visitor Center. "Walking Tour of Historic Downtown Corsicana." On page four, the tale of the wandering Jewish rope walker. Good Lord, Nancy, listen to this. At dusk, if no one's down there working, I'll descend to the second floor and stand for a while in the southeast corner where Doug usually spent his spare time. With windows open on two sides. There is a Main Street, but the real main street is Beat on Street which runs along the east side of the building. From the south side's east-most window - right behind Doug as he worked - you get

Figure 33: Top-activating examples for a feature in FF-KV annotated as “conceptual”. The specific annotation was “concept related to the coast” especially in various contexts.

Text ID: 5531 (Max Activation: 2.516)

ingredients ! Course : Sweet / dessert Cuisine : Indian Serv ings : 2 0 kaj u kat lis Calories : 8 3 kcal Author : Har

ini Ingredients ( 1 cup = 2 5 0 ml ) 1 cup cas hews 1 cup powdered sugar 1 / 8 teaspoon saffron optional 1 / 2  
 teaspoon cardamom powder Instructions Soak cas hews in water for 3 0 minutes . Powder the sugar . Grind cas hews to  
 a very fine paste , just y sprinkling water . Measure one cup of ground cashew paste and powdered sugar and take in a  
 non stick pan . Mix well . Now heat the mixture over low - medium flame and start to

Text ID: 5528 (Max Activation: 2.406)

. keep sc arp ing the sediments while stirring . Add saffron and mix well . 5 . Keep stirring for 7 - 1 0 minutes , The  
 kaj u sugar mixture will start bubbling and it will begin to thicken . Make sure to scrape the edges while stirring .

Add saffron at this stage if you want to add . 6 . Once the kaj u sugar mixture forms a lump and gathers in the  
 center , pinch a very small amount and make a ball with your fingers . if you are able to form a ball , then it is the correct  
 consistency . Switch off the flame and let the mixture cool for a while . 7 .

Text ID: 5530 (Max Activation: 2.297)

be very thin , so roll the dough as thin or thick as you prefer . 9 . Allow the pieces to set for 1 0 minutes .

Store kaj u kat lis airtight in room temperature . If you refrigerate the kaj u kat lis may turn a bit hard . Kaju kat li  
 recipe card below : 5 from 6 votes Print Kaju kat li recipe , cashew fudge recipe | how to make kaj u kat li Prep  
 Time 3 0 mins Cook Time 1 0 mins Total Time 4 0 mins Kaju kat li recipe is a royal Indian sweet , vegan  
 cashew fudge , rich melt in mouth with just

Text ID: 5533 (Max Activation: 2.203)

1 0 minutes . Store kaj u kat lis airtight . Recipe Notes 1 . Do not add more water while grinding . Just sprinkle to  
 ease the grinding , the cashew paste should be very smooth . 2 . Do not cook the mixture more than 1 0 minutes .  
 Once the lump reaches soft ball stage , remove from flame . The mixture will further thicken when it cools . 3 . Kne  
 ad the mixture very well but gently , the more you kne ad the more soft your kaj u kat lis will be . 4 . If the dough  
 seems to be dry you can a tablespoon of milk or water while kne ading . Sharing

Figure 34: Top-activating examples for a feature in  $k$ -Sparse FF-KV annotated as “conceptual”. The specific annotation was “concept related to recipes” especially in contexts related to deserts.

Text ID: 14508 (Max Activation: 14.855)

I did with the Codex . WI RED : How do you deal with technology ? Sera fini : I remember my first encounter with a tablet . I was working on the opening titles of two Italian television broadcasts , Onda Verde and Enzo Biagi ' s La Lunga Marcia about his journey through **China** . It was a new tool , wired to a giant - size computer – quite fascinating at the time . I used it recently to illustrate Nature Stories by Jules Renard , but

I realized my hand is much quicker . WI RED : Another encyclopedia of nature . Are you somehow obsessed with that kind of book ? Sera fini :

Text ID: 6117 (Max Activation: 13.967)

right , are John Home Tooke another radical MP and Catharine Macaulay . She , like the other women , wears French tricolours . The people in this print are all linked by their support for the Revolution . The women were distinguished for refuting Burke in print , or so it seemed . Williams who was noted for her sympathetic , eyewitness Letters Written in **France** had just published a poem in praise of the storming of the Bastille . Catharine Macaulay ' s forthcoming attack on Burke ' s Reflections had been announced and Barbauld , who had first opposed Burke in March 1790 , was assumed to be writing another refutation of his Reflections . While

Text ID: 13267 (Max Activation: 13.466)

and political risks which UK businesses may face when operating **abroad** , including **in Israel and** the **OPT s** . This includes guidance on Israeli settlements . We are advising British businesses to bear in mind the British Government ' s view on the illegality of settlements under international law when considering their investments and activities in the **region** . This is voluntary guidance to British businesses on doing business in **Israel and OPT s** . Ultimately it will be the decision of an individual or company whether to operate in settlements in the Occupied **Territories** , but the British Government would neither encourage nor offer support to such activity . When approached by businesses , we set out the UK ' s clear position on

Text ID: 9248 (Max Activation: 13.382)

the official said . Manchester United goalkeeper Sam Johnstone is poised to rejoin Aston Villa on Monday . The 24 - year - old has been a target for a number of Championship and Premier League sides but will sign for Villa on a season - long loan . Johnstone , who spent the second half of last season on loan at Villa Park , still has another year left on his contract at United after this one . Manchester United goalkeeper Sam Johnstone is poised to rejoin Aston Villa on Monday He has been back in training at United ' s Carrington complex and will not be part of the **tour** party that travels **to the USA on**

Text ID: 7155 (Max Activation: 13.311)

980 s , Evergreen transported U . S . troops on drug raids in **Central and South America** , the paper said . Over the years , company officials denied working for the CIA . When contacted Wednesday by The Providence Journal to discuss Evergreen ' s relationship with the CIA , a spokesman for the spy agency declined to comment . The company also had contracts to carry U . S . Mail , as well as transporting cargo and personnel for private businesses . Evergreen filed for liquidation under Chapter 7 of the U . S . Bankruptcy Code on Dec . 31 , 2013 , in the Delaware District .

Figure 35: Top-activating examples for a feature in SAE annotated as “conceptual”. The specific annotation was “name of country and region” in various contexts.

**Text ID: 1508 (Max Activation: 27.375)**

during his tenure . He served as co - offensive coordinator at Cata w ba College from 2 0 0 2 - 0 4 and offensive coordinator at Delta State from 2 0 0 6 - 0 6 . A 1 9 9 9 graduate of Florida State with a bachelor ' s degree in sports management , Bloom gren earned his master ' s degree in higher education from Alabama in 2 0 0 1 . A native of Tallahassee , Florida , Mike and his wife , Lara , have two sons , Tyler and Parker . The Bloom gren File Hometown : Tallahassee , Florida College : Florida State , 1 9 9 9

**Text ID: 7547 (Max Activation: 25.625)**

active in spreading the relevance and importance of this technology as it helps promote economic freedom . He was formerly Head of Research at Brave New Coin ( http :// bra ven ew coin . com / authors / tone - v ays / ) after previously writing about trading and economics at Coin Tele graph ( https :// co intele graph . com / authors / tone \_ v ays ) . Tone maintains a personal website Liberty Life Trail where you can find his latest research on Bitcoin , Blockchain , sound economics and privacy . Tone holds a Masters Degree in Financial Engineering from Florida State University along with Bachelor Degrees in Mathematics and Geology . 8 : 0 0 pm ( 3 0 minutes

**Text ID: 4722 (Max Activation: 24.750)**

He graduated from Texas A & M University with a B . S in Agricultural Education and a Master of Education degree . Tom likes being his own boss so he can take off to go fishing , whenever he likes , and leave his wife in charge of the business . Email Tom at les ter 0 1 @ air mail . net Visit Tom at his web site : Fishing Pro Staff MUM BAI / DEL HI : R itesh Srivastava speaks with the ferv our of a true believer . " I am a li fer here . The work and systems are as professional as any other FMC G company . But the work culture and what the brand stands for

**Text ID: 334 (Max Activation: 24.375)**

impacting the lives of low - income working families . Minimum - wage research should be conducted with the best feasible study designs , just as federal agencies demand the best designs when they seek out evaluations of other labor market policies . About the author Daniel Kue hn is a doctoral student in American University ' s Department of Economics with field special izations in labor economics and gender economics . Before coming to American University he was a research associate at the Urban Institute ' s Center on Labor , Human Services , and Population . He has a master ' s degree in public policy , specializing in labor market policy , from George Washington University . Acknowledgements The paper

Figure 36: Top-activating examples for a feature in **Transcoder** annotated as “conceptual”. The specific annotation was “concept related to college degrees” in various contexts.

Text ID: 1669 (Max Activation: 0.746)

s specialized in **Dark** moves **so maybe** I'll ... Oh **dear God** what have I become? **They** got me. I'm **hooked on** **Pokémon** and I **didn't** even see it coming. Strange how much a **good** motivator can improve a **game's** overall appeal. Suddenly **the arena battles weren't** so pointless; I was **working towards something**. **Collecting Pokémon started to matter** because **the more powerful ones could help me beat challenges to get** more points to upgrade **Zoro ark**. My **Zoro ark**. **My precious ... Beyond the storyline mode that can be beat in** roughly six **hours of playtime**, **there are tons of little** motivators built

Text ID: 5179 (Max Activation: 0.691)

feasible **that the organisation** may announce some kind of second **Season Pass**, **assuming** that the **player** base is still **there**. **Whatever the case**, a **new** patch will deploy **next week**, adding **Elite Driver levels**, **improvements to the title's Photo Mode**, and much more. Where would you **like** to see the **game** go next? Take a **sharp** hairpin turn in **the** comments section below. **Melania Trump's official White House portrait has been released. Here it is.** **And ... she looks like a** model. **Probably because she** used to be one. **So?** **The Boston Globe** immediately picked **the whole thing** apart top to bottom.

Text ID: 9857 (Max Activation: 0.664)

relatives of the **hospital's** medical, nursing and administrative personnel. Among them five refused to **participate**, **whereas five** had **mini-mental examination scores < 23** and **therefore were excluded** from the study. **Thus**, the control **group** consisted of **110 HCs (103 females / 7 males)** unrelated to the **patients who were age - sex matched with the p** **SS group**. **Exclusion criteria included** the presence of autoimmune **disease**, neuro psychiatric history, use of psychotropic drugs, alcoholism and drug **abuse**. The **first part of the questionnaire addressed the main demographic characteristics** as well as smoking and drinking habits. The **second part of the**

Text ID: 12993 (Max Activation: 0.645)

role in supporting **the** newcomers at 100W, even as **the arts** council hasn't embraced Hob rats chik and company in the same way. The arts council is more focused **on arts education in** Navarro County **schools than producing or displaying art** these days, Brooks said. "It makes no sense," he said. "I'm an old educator, so I get doing it **for the kids**", but there are **adults** with artistic talent **that need to be nurtured**." In **his** study at home, Brooks keeps a caricature someone made of him back when he was helping start the arts council. The character is pulling a wagon full of **statues**

Figure 37: Top-activating examples for a feature in FF-KV annotated as "Uninterpretable".

**Text ID: 7567 (Max Activation: 0.676)**

). I suggest that this filter plays a significant role in explaining the different patterns of deference exhibited by conservatives and liberals . The disposition to defer to others with whom we share a political or religious outlook is continuous with the disposition to use benevolence as a cue to reliability ; we are disposed to see those with whom we share a political outlook and / or a religious affiliation as those who are benevolent toward us and our interests ( or , perhaps , the disposition to use benevolence as a cue to reliability is just a special case of a disposition to defer to those with whom we share values ). The use of political and religious affiliation as a proxy for benevolence is

**Text ID: 7727 (Max Activation: 0.609)**

, I don ' t even know who Thomas Mars is and I never have the phone records ," Robertson said . " I never find that call ." Tens of thousands of Roman ians and Bulg arians have come to the UK to work since restrictions were lifted Peter Nicholls / The Times Net migration has reached a record 3 3 6 , 0 0 0 as figures published yesterday showed that Roman ians are now the third biggest group coming to the UK . Officials said the latest increase was driven by a " stat istically significant " rise in the overall number of immigrants , with many of them arriving to take up jobs . The surge was partly because

**Text ID: 8655 (Max Activation: 0.605)**

Iran threat . Check out the full segment below . He is now one of five active coaches in the ACC and one of 1 5 active coaches in DI to accomplish the feat . R ALE IGH , N . C . – NC State baseball head coach Elliott Avent recorded his 1 , 0 0 0 th career win against North Carolina Central Tuesday evening , as the Wolf pack hit a season - high four home runs en route to a 1 3 - 0 win at Do ak Field at D ail Park . Now in his 2 8 th season as a head coach and 2 1 st at NC State , Avent

**Text ID: 5332 (Max Activation: 0.605)**

. They reported that Einstein was right . Since then , his theory has been ret ounded in detail , but its essentials have been repeatedly verified . No important scientist is to be found among the skept ics , although there is every incentive to deb unk Einstein , if it can be done . Immort ality awaits the man who can overthrow Einstein . The popular uproar over the theory surprised no one more than the author of the theory . He had been almost a reclu se . His contacts had been with quiet , scholarly men of his own type , and his sudden glory appalled him . Interview ers , photographers , lion - hunters , cause - prom oters , testimonial

Figure 38: Top-activating examples for a feature in *k*-Sparse FF-KV annotated as “Uninterpretable”.

**Text ID: 15344 (Max Activation: 4.632)**

Aaron Gle eman of Hard ball Talk ) reports C . K . purchased an East End mansion that Babe Ruth spent time at .  
Ke il reports the comedian shelled out \$ 2 . 4 9 million for the 4 , 9 5 7 - square foot " Prim rose Cottage " formerly visited by the New York Yankees legend . The home is a three - story Tudor originally constructed in 1 9 0 1 with six bedrooms , three - and - a - half baths and five fireplaces . Yes , there are more fireplaces than bathrooms in this home , which is probably a zoning requirement in the Ham ptons ( or one of Ruth ' s ecc entri

**Text ID: 12336 (Max Activation: 4.299)**

the new ones . Additionally , ssh server key theft is another one - time vector that can be used to quickly bootstrap into node key theft . For this reason , node admins should always use ssh key auth for tor node administration accounts , since it prevents ssh server key theft from implying continuous server compromise : http :// www . gre m well . com / ssh - mit m - public - key - authentication Issues With Ephe meral Identity Keys There are a few issues with deploying ephemeral identity keys . Issues With Ephe meral Identity Keys : Client guard node loss The primary issue with ephemeral identity keys is client Guard node loss . If your relay obtains the Guard flag

**Text ID: 8158 (Max Activation: 4.289)**

given Trump ' s sharp criticism and talk of " re visiting " the Iran nuclear deal . The message is loud and clear :  
The United States cannot be trusted . Third , the U . S . - South Korean alliance is not impenetrable . President Trump tweeted his criticism about the South Korea - United States free trade agreement around the time of the 4 th nuclear test and accused the South Korean government of " appea sement with North Korea ." South Korea is finding , as I have told them , that their talk of appea sement with North Korea will not work , they only understand one thing ! — Donald J . Trump (@ real Donald Trump

**Text ID: 4557 (Max Activation: 4.193)**

```
specifically does is somewhat meaningless and arbitrary . struct Table Based Sorter { Table Based Sorter ( const int values [ 1 2 8 ] ) { for ( int i = 0 ; i < 1 2 8 ; ++ i ) m Table [ i ] = (( values [ i ] ^ 0 xff 8 0 ) + 1 2 8 ) - i ; } bool operator ()( int a , int b ) const { return m Table [ b ] < m Table [ a ] ; } int m Table [ 1 2 8 ] ; } ;  
std :: sort ( v , v + 1 2 8 , Table Based Sorter ( values ) ); The
```

Figure 39: Top-activating examples for a feature in SAE annotated as “Uninterpretable”.

Text ID: 9130 (Max Activation: 7.969)

, but their authors are well - re know ned . Linear Systems and State - Space Sorry , I don ' t have anything I can recommend here ; what I ' ve read is either mediocre or falls deeply into theoretical matrix hell without really coming up for air . ( The Dahleh s at MIT fall into this latter category .) Linear Systems Theory by João P . Hes pan ha may be of use . Chapter 1 is freely available online , and I found it useful for the various state - space inter connections . But it looks like a typical textbook over reliance on MATLAB . Oh , and I can ' t stand the heading

Text ID: 10600 (Max Activation: 7.719)

ulus AG . The announcement was made official by John Han ke , Director of Google Earth & Maps . Stefan and Bruno Mu ff founded End ox on . A large number of the employees of End ox on are still with Google working as Software Engineers , Managers , and V Ps . 3 6 . 4 % of Xun lei ( Price : \$ 5 million , Date : January 4 , 2 0 0 7 ) X un lei is a Chinese file - sharing website that supports Bit Torrent , FTP , e Donkey , etc . Xun lei was developed by Thunder Networking Technologies and is based in the southern province of Shenzhen . Xun

Text ID: 6250 (Max Activation: 7.469)

: \$ 1 3 5 billion for medical care and benefits of Iraq and Afghan war veterans . An estimated \$ 7 4 3 billion in additions to the Pentagon ' s base budget . Although these funds were not spent directly in the war theaters , the researchers believe they would not have been appropriated had the wars not been undertaken . \$ 4 5 5 billion for homeland security . Again , the assumption is made that much or all of this spending would not have been undertaken but for the war and climate of war . \$ 1 3 0 billion in additional spending on war operations and war - related base budget for 2 0 1 4 .

Text ID: 15443 (Max Activation: 7.406)

remaining cards in the deck in the middle of the playing area . Leave room next to the deck for a discard pile . Third , deal out the Recipe cards , face - up , into card piles in the center of the playing area . The number of piles will be one more than the total number of players . For example , if playing a game with four players , there will be five Recipe piles . Fourth , take the Season cards and put them in their proper order ( Spring , Summer , Fall , and then Winter ) . Select a season to start with and place this card face - up . The Season deck should remain face -

Figure 40: Top-activating examples for a feature in **Transcoder** annotated as “Uninterpretable”.

## FF-KV

4 5 . 3 0 0 naar 1 3 0 . 0 0 0 ( ter wijl de te werks telling voor Bel gen met 1 6 . 0 0 0 een heden da alde ). Ten tweede is het op mer kelijk dat er tussen 2 0 1 1 en 2 0 1 5 – de nad agen van de financi ële crisis met nog beho or lijk wat werk lo zen - in ons land meer ban en zijn gescha pen voor gede ta cheer den dan voor Bel gen : 6 5 . 0 0 0 Bel gen kre gen een nieuwe baan als lo ont rek kende of zelf stan dige , tegen 8 7 .

## Transcoder

4 5 . 3 0 0 naar 1 3 0 . 0 0 0 ( ter wijl de te werks telling voor Bel gen met 1 6 . 0 0 0 een heden da alde ). Ten tweede is het op mer kelijk dat er tussen 2 0 1 1 en 2 0 1 5 – de nad agen van de financi ële crisis met nog beho or lijk wat werk lo zen - in ons land meer ban en zijn gescha pen voor gede ta cheer den dan voor Bel gen : 6 5 . 0 0 0 Bel gen kre gen een nieuwe baan als lo ont rek kende of zelf stan dige , tegen 8 7 .

Crossing : New Leaf am iibo cards will also become available for purchase . No matter how you play it , this is the perfect time to cozy up to the charm and creativity of this special game . New friends and discoveries await every day . Express yourself by customizing your character , home , and town as you create your ideal world . The arcade : the last bastion of loose change . Or so we thought . An old - school arcade , in the retirement capital of New Zealand no less , complete with Pac - Man , pinball and teddy bear claw machines , has started using cryptocurrency . And actually , it ' s not that cryptic .

Crossing : New Leaf am iibo cards will also become available for purchase . No matter how you play it , this is the perfect time to cozy up to the charm and creativity of this special game . New friends and discoveries await every day . Express yourself by customizing your character , home , and town as you create your ideal world . The arcade : the last bastion of loose change . Or so we thought . An old - school arcade , in the retirement capital of New Zealand no less , complete with Pac - Man , pinball and teddy bear claw machines , has started using cryptocurrency . And actually , it ' s not that cryptic .

. 0 0 0 0 0 0 0 0 e + 0 0 - 1 . 0 6 5 8 1 4 1 0 e - 1 4 - 8 . 5 2 6 5 1 2 8 3 e - 1 4 - 1 . 1 3 6 8 6 8 3 8 e - 1 3 1 . 0 0 0 0 0 0 0 0 e + 0 2 ] ] den = [ 1 . 1 8 . 9 7 . 1 8 0 . 1 0 0 . ] cond ( A ) = 1 0 . 0

The modal form expresses any state - space system as the parallel sum of separate first - order systems

. 0 0 0 0 0 0 0 0 e + 0 0 - 1 . 0 6 5 8 1 4 1 0 e - 1 4 - 8 . 5 2 6 5 1 2 8 3 e - 1 4 - 1 . 1 3 6 8 6 8 3 8 e - 1 3 1 . 0 0 0 0 0 0 0 0 e + 0 2 ] ] den = [ 1 . 1 8 . 9 7 . 1 8 0 . 1 0 0 . ] cond ( A ) = 1 0 . 0 The modal form expresses any state - space system as the parallel sum of separate first - order systems

Figure 41: The first feature pair we annotate as **aligned**.

## FF-KV

```

the timer cuda Event Record ( stop , 0 ); cuda Event Synchron ize ( stop ); //
Copy scaled image to host cud asa fe ( cuda Mem cpy ( new Pixels , new
Pixels _ dyn , new Image Byte Length , cuda Mem cpy Device To Host )," from
device to host ", __ FILE __ _ LINE __ ); new Image -> pixels = new Pixels ; //
Free memory cuda Free ( pixels _ dyn ); cuda Free ( new Pixels _ dyn ); cuda
Event Elapsed Time ( & time , start , stop ); printf ( " Time for the kernel : % f
ms " , time ); // Save image SDL _ Save BMP ( new Image , " test

```

```

h ; // Create pointer to device and host pixels Uint 8 * pixels = ( Uint 8 * )
image -> pixels ; Uint 8 * pixels _ dyn ; cuda Event _ t start , stop ; float time ;
cuda Event Create ( & start ; cuda Event Create ( & stop ); // Copy original image
cud asa fe ( cuda Malloc ( ( void ** ) & pixels _ dyn , image Byte Length ),"
Original image allocation ", __ FILE __ _ LINE __ ); cud asa fe ( cuda Mem cpy (
pixels _ dyn , pixels , image Byte Length , cuda Mem cpy Host To Device ),"
Copy original image to device ", __ FILE __ _ LINE __ ); // Allocate new image
on

```

```

blue ; } 1 1 . Save image After saving an image , we would like to keep
environment clean , so deal locate memory by cuda Free function . // Copy
scaled image to host cud asa fe ( cuda Mem cpy ( new Pixels , new Pixels _ dyn
, new Image Byte Length , cuda Mem cpy Device To Host )," from device to host
", __ FILE __ _ LINE __ ); new Image -> pixels = new Pixels ; // Free memory
cuda Free ( pixels _ dyn ); cuda Free ( new Pixels _ dyn ); // Save image SDL _
Save BMP ( new Image , " test 2 . bmp "); // Free surfaces SDL _ Free

```

```

), with a massive lead on Harper ( 1 5 per cent ) and a comfortable lead
over Trudeau ( 2 5 per cent ). The telephone poll sampled 1 3 9 2
randomly selected voters across the country on Aug . 1 0 - 1 1 . It is
considered accurate to within plus or minus three percentage points , 1 9
times out of 2 0 . @ Josh _ F is on Twitter . Remember for instant
breaking news follow @ cp 2 4 on Twitter . Mitt Romney ' s advantage among
male voters has all but disappeared since the Democratic National Convention .
The pattern will likely spell doom for Romney unless it

```

## Transcoder

again and I recommend the company . Yes , I recommend this product . Verified  
Purchase . I recommend this product . A very pleasant surprise I was very  
skeptical when I first ordered this jacket but I ' m a HUGE fan of Star Wars  
and I had to take a chance . Well that chance paid off . This jacket is  
amazing . It really is real leather , it fits like a glove . I don ' t know what else  
to say . The shipping took a little longer than I anticipated , but I placed  
my order around Christmas . When I did contact their customer support they  
responded very quickly and assured me it would ship as soon as it

to it . Alright then , thanks so much guys for an amazing jacket and superb  
service . Be sure to hear from me again soon . I would surely come back for  
more ; ) Yes , I recommend this product . Verified Purchase . I recommend this  
product . Great quality and excellent service . The jacket is of really great  
quality and is very comfortable to wear . The delivery has been lightning fast  
and the support team has been of great help regarding sizing and so on .  
Highly recommended you will not regret it . Yes , I recommend this product .  
Verified Purchase . I recommend this product . Can ' t complain except that it ' s

Yes , I recommend this product . Verified Purchase . I recommend this product .  
Great quality , quick delivery The jacket is near identical to the actual thing ,  
high quality materials and feels sturdy . Delivery was great , went with the  
cheapest delivery option and it arrived to me in the uk in 5 days . The  
jacket fits well in the chest and is a good length , only problem I have is it is  
very tight on the upper arms around the arm pit / del toid area Yes , I recommend  
this product . Verified Purchase . I recommend this product . OH . MY . GOD .  
Seriously , you have no idea how happy you made

2 2 nd birthday . He is a huge Star Wars fan and had shown it to me before  
. When he opened his gift and saw it he was in shock ! It is so well made  
and fits perfectly and didn ' t think I had gotten it for him . This jacket is  
gorgeous and the customer service is amazing ! It arrived quicker than  
expected . I highly recommend this company and jacket for any Star Wars fan  
. Yes , I recommend this product . Verified Purchase . I recommend this product .  
I love this jacket so much To any customer that is thinking about purchasing  
this jacket I am a verified happy customer . I have ordered multiple

Figure 42: The first feature pair we annotate as **un-aligned**.